PHILOSOPHICAL TRANSACTIONS OF THE ROYAL SOCIETY A MATHEMATICAL, PHYSICAL & ENGINEERING SCIENCES

Linear Global Modes in Spatially Developing Media

Stephane Le Dizes, Patrick Huerre, Jean Marc Chomaz and Peter A. Monkewitz

Phil. Trans. R. Soc. Lond. A 1996 **354**, 169-212
doi: 10.1098/rsta.1996.0006

Linear global modes in spatially developing media

By Stéphane Le Dizès[1]†, Patrick Huerre[1], Jean Marc Chomaz[1] and Peter A. Monkewitz[2]

[1] *Laboratoire d'Hydrodynamique (LadHyX), Ecole polytechnique, F-91128 Palaiseau cedex, France*

[2] *Département de Mécanique, IMHEF, Ecole Polytechnique Fédérale de Lausanne, ME-Ecublens, CH-1015 Lausanne, Switzerland*

Contents

Selection criteria for self-excited global modes in doubly infinite one-dimensional domains are examined in the context of the linearized Ginzburg–Landau equation with slowly varying coefficients. Following Lynn & Keller (1970), uniformly valid approximations are sought in the complex plane in a region containing all relevant turning points. A mapping transformation is introduced to reduce the original Ginzburg–Landau equation to an exactly solvable comparison equation which qualitatively preserves the geometry of the Stokes line network. The specific case of two turning points with counted multiplicity is analysed in detail, particular attention being paid to the allowable configurations of the Stokes line network. It is shown that all global modes are either of type-1, with two simple turning points connected by a common Stokes line, or of type-2, with a single double-turning point. Explicit approximations are derived in both instances, for the global frequencies and associated eigenfunctions. It is argued, on geometrical grounds, that type-1 global modes may, in principle, be more unstable than type-2 global modes. This paper is a continuation

† Present address: IRPHE, 12 avenue Général Leclerc, F-13003 Marseille, France.

Phil. Trans. R. Soc. Lond. A (1996) **354**, 169–212
Printed in Great Britain

and extension of the earlier study of Chomaz, Huerre & Redekopp (1991), where only type-2 global modes were investigated via a local WKBJ approximation scheme.

1. Introduction

Several classes of spatially developing shear flows are known to exhibit, under certain flow conditions, self-sustained oscillations: the near field large-scale dynamics become effectively tuned at a specific intrinsic frequency, the associated spatio-temporal distribution of fluctuations defining a *global mode* of the flow. The main objective of the present study is the systematic derivation of global frequency selection criteria in the context of the linearized Ginzburg–Landau model equation with varying coefficients. It should be viewed as a continuation and extension of the analysis presented in Chomaz *et al.* (1991) for the same model problem.

Some of the underlying physical motivation and key stability concepts are now briefly recalled. The reader is referred to the recent surveys by Huerre & Monkewitz (1990) and Monkewitz (1990) for extensive discussions on theoretical and experimental aspects of global mode evolution in shear flows. The onset of the Kármán vortex street in the flow behind a bluff cylindrical body probably constitutes the primary example of transition to a global mode regime: as the Reynolds number exceeds a critical value, the wake develops limit cycle oscillations that arise via a Hopf bifurcation, as documented extensively by Mathis *et al.* (1984), Hannemann & Oertel (1989), Karniadakis & Triantafyllou (1989) and Strykowski & Sreenivasan (1990), among others. Current research on wake flow stability is compiled in a book of proceedings by Eckelmann *et al.* (1993). As shown in the experiments of Sreenivasan *et al.* (1989) and Monkewitz *et al.* (1990), a similar phenomenon takes place in the near field region of jets, when the jet density is gradually decreased below that of the surrounding medium. Beyond a critical density ratio, the evolution of vortical structures becomes highly repeatable in the first few diameters downstream and frequency spectra collapse into discrete peaks as one would expect in the presence of a global mode. As a last example, one should mention the ingenious experiments of Strykowski & Niccum (1991) which conclusively demonstrate the existence of global modes in counterflow mixing layers for sufficiently high velocity ratios. The occurrence of intrinsic oscillations therefore appears to be ubiquitous in many spatially developing shear flows.

From a stability point of view, the most elementary approach consists in entirely neglecting the spatial development of the medium: if the basic flow is assumed to be uniform in the propagation direction, the stability properties of normal modes $\exp\{(\mathrm{i}(kx-\omega t)\}$ are completely described by a dispersion relation $D[k,\omega]=0$ between wavenumber k and frequency ω. The ability of perturbations to grow in time at the source, in response to a localized impulse, is characterized by the absolute growth rate $\omega_{0,\mathrm{i}} \equiv \mathrm{Im}\,\omega_0$, where the complex absolute frequency $\omega_0 \equiv \omega(k_0)$ is defined by the usual group velocity condition

$$\frac{\mathrm{d}\omega}{\mathrm{d}k}(k_0)=0.$$

If $\omega_{0,\mathrm{i}}<0$, any temporally amplified perturbation leaves its source and the medium is said to be convectively unstable. If $\omega_{0,\mathrm{i}}>0$, there exist perturbations that will grow *in situ* at the source and the medium is said to be absolutely unstable. A more

comprehensive account of these concepts may be found, for instance, in Bers (1983) as well as in the previously quoted survey articles.

Most basic flows of interest are spatially non-uniform in the propagation direction x as a result of viscous diffusion or boundary effects. The previous notion can then be taken to apply locally in x, as long as the non-uniformities of the medium are small over a typical wavelength of the instability. Thus the non-parallelism of the flow is characterized by a slow space scale $X = \varepsilon x$, where ε is a small parameter of the same order of magnitude as the scaled non-uniformities. Decomposition into local normal modes leads to a dispersion relation of the form

$$D[k, \omega; X] = 0. \tag{1.1}$$

The flow is then defined to be *locally* stable, convectively unstable or absolutely unstable at a given station X in the same manner as for the uniform case. The entire medium is therefore partitioned into different domains, according to the local nature of the instability. One can then attempt to establish a link between the experimentally observed global response of the flow and the calculated streamwise distribution of local stability properties, in particular the extent of different regions of convective and absolute instability. Such an approach has effectively been implemented for several classes of spatially developing flows, among them wakes (Koch 1985; Monkewitz 1988; Hannemann & Oertel 1989; Schär & Smith 1993), low-density jets (Monkewitz & Sohn 1988; Monkewitz *et al.* 1990) and counterflow mixing layers (Strykowski & Niccum 1991). In all three cases, there are ranges of control parameter, i.e. Reynolds number, density or velocity ratio, in which the basic state is convectively unstable everywhere. Such flows are known to behave primarily as spatial amplifiers of external noise: if forcing is turned off they return to the basic state and are therefore globally stable. In other parameter ranges, global intrinsic oscillations are found to develop concurrently with the appearance of a sufficiently large pocket of local absolute instability.

In order to introduce global model concepts, dispersion relation (1.1) is formally rewritten in physical space as a partial differential equation

$$D\left(-\mathrm{i}\frac{\partial}{\partial x}, \mathrm{i}\frac{\partial}{\partial t}; X\right) \Psi(x, t; \varepsilon) = 0, \tag{1.2}$$

for the perturbation field $\Psi(x, t; \varepsilon)$. Following Huerre & Monkewitz (1990) and Chomaz *et al.* (1991), a global mode is then defined as a solution of (1.2) which is temporally harmonic, of complex frequency ω_{g} and satisfies, say, exponential decay conditions at $X = \pm\infty$. Upon making the substitution

$$\mathrm{i}\frac{\partial}{\partial t} \rightarrow \omega_{\mathrm{g}}$$

in (1.2), the determination of global modes is effectively reduced to an eigenvalue problem in the propagation direction X. Our present understanding of the global mode problem has often relied on the study of the Ginzburg–Landau equation with varying coefficients as a simple model for the operator D in (1.2). Global instability concepts appear to have first been introduced by Drazin (1974*a*) for a particular version of the linearized Ginzburg–Landau equation containing no advection term and with purely real coefficients. The model therefore exhibited reflectional symmetry and attention was restricted to real turning point configurations. In the purely one-dimensional context, Chomaz *et al.* (1988) demonstrated at an early stage, through a combined analytical and numerical approach, that a necessary condition for global

instability is the existence of a region of local absolute instability of finite extent. Hunt (1995) has further shown that this condition is indeed not sufficient: for an *ad-hoc* Ginzburg–Landau model, the basic state can be made absolutely unstable everywhere while the medium remains globally stable. Following the seminal studies of Gent (1974), Gent & Leach (1976), Soward & Jones (1983), Pierrehumbert (1984) and Koch (1985), Chomaz *et al.* (1991) investigated global frequency selection on the Ginzburg–Landau model on a doubly infinite domain. As in the present case, the primary objective was the derivation of a criterion expressing the global frequencies $\omega_{\rm g}$ solely in terms of the properties of the local dispersion relation (1.1). The global mode structure along the propagation direction was sought in the form of WKBJ expansions satisfying appropriate exponential decay conditions at $X = +\infty$ and $X = -\infty$, respectively. The ability to construct an analytic eigenfunction with such prescribed WKBJ expansions led to definite constraints on the configuration of Stokes lines associated with each turning point in the complex X plane. Thus, it was possible to prove, albeit incompletely as we shall see, that global growth rates $\omega_{\rm g,i} \equiv \mathrm{Im}\,\omega_{\rm g}$ cannot exceed the maximum absolute growth rate $\omega_{0,\rm i}^{\rm max}$ on the real X-axis. A convectively unstable medium is therefore necessarily globally stable. Furthermore, under specific assumptions regarding the nature of the turning points and the properties of the complex function $\omega_0(X)$, the WKBJ approximations near $X = +\infty$ and $X = -\infty$ could be matched to an inner turning point solution for only a discrete collection of global frequencies $\omega_{{\rm g}_n}$. At leading order in ε, all global frequencies were found to be determined by the value $\omega_{\rm s} \equiv \omega_0(X_{\rm s})$ of the absolute frequency at the saddle point $X_{\rm s}$ such that

$$\frac{{\rm d}\omega_0}{{\rm d}X}(X_{\rm s}) = 0.$$

Hunt & Crighton (1991) have recently devised an elegant procedure to calculate exactly the Green function of the Ginzburg–Landau equation with varying coefficients. For quadratic variations of $\omega_0(X)$, the long-time behaviour of the Green function is shown to reduce to the most unstable global mode of leading-order global mode frequency $\omega_{\rm s}$. This result fully confirms that the frequency selection criterion of Chomaz *et al.* (1991) is indeed causal and naturally emerges from the impulse response.

It should be emphasized that several real fluid flow configurations have already been analysed from the global mode point of view: the Kelvin–Helmholtz instability of a vortex sheet of varying strength in the spanwise direction (Drazin 1974*b*), the Taylor vortex problem between two eccentric rotating cylinders (DiPrima & Stuart 1972) or between two concentric spheres (Soward & Jones 1983), baroclinic instabilities in geophysical flows (Gent 1974; Gent & Leach 1976; Pierrehumbert 1984; Bar-Sever & Merkine 1988), unsteady viscous flow in a curved pipe (Papageorghiou 1987), thin-disc dynamo models (Soward 1992) and, most recently, spatially developing shear flows (Monkewitz *et al.* 1993). In this regard, the combined experimental and theoretical study of Gent & Leach (1976) strikingly demonstrated that global modes can be observed in baroclinically unstable flow in an eccentrically mounted differentially heated rotating annulus. The present study is further motivated by the fact that, in many of these investigations, the Ginzburg–Landau model with varying coefficients rationally arises as the leading-order governing equation in the turning point region.

The primary goal of this work is to examine anew the global frequency selection criterion derived in Chomaz *et al.* (1991) by resorting to a different formulation, namely the method of uniform approximations. This approach, which has been in-

troduced and developed by Langer (1949), McKelvey (1955), Lynn & Keller (1970) and Anyanwu & Keller (1975) among others, relies on the following idea: one seeks to determine approximations to the global mode structure that remain uniformly valid in the entire domain of interest including all relevant turning points as well as the boundaries $X = \pm\infty$. Through an appropriate transformation applied to the dependent and independent variables, the original problem is reduced to a so-called comparison equation that can be solved exactly. All the art of the method resides in the careful selection of a mapping which preserves the topological properties of the initial Stokes line network. The global frequencies are directly obtained from the known solutions of the comparison equation, and the associated spatial eigenfunctions are expressed in terms of a single uniformly valid approximation.

The paper is organized in the following manner. The global mode problem for the Ginzburg–Landau model is stated in § 2, together with essential definitions and properties of turning points and Stokes lines. In order for a global mode to exist, the corresponding Stokes line network should be restricted to specific configurations as demonstrated in § 3. Unfortunately these necessary conditions only lead to exclude a small set Δ_0 of Stokes lines from consideration. The general method of uniform approximations in the version proposed by Lynn & Keller (1970) is outlined in § 4 for an arbitrary number of turning points. The bulk of the study is presented in § 5 for the specific case of two turning points. The properties of the transformation leading to the comparison equation are first analysed in detail. In particular, it is argued in § 5 *b* that the Stokes sectors containing $X = +\infty$ and $X = -\infty$, respectively, cannot be contiguous for large $|X|$ if ω is to give rise to a global frequency. Upon solving the comparison equation in the mapped domain, global modes are then shown (§ 5 *c* and *d*) to fall within only two classes: type-1 modes correspond to two simple turning points connected by a Stokes line and type-2 modes to a double-turning point. The resulting extended frequency selection criteria are discussed and interpreted geometrically in § 5 *e*. In closing, we summarize the main conclusions of the study and compare them with available numerical and experimental evidence.

2. Basic formulation

As in Chomaz *et al.* (1991), complex scalar fluctuations $\Psi(x,t)$ around a given basic state are assumed to be governed by the linearized Ginzburg–Landau equation

$$\left[\mathrm{i}\frac{\partial}{\partial t} + \frac{1}{2}\omega_{kk}(X)\frac{\partial^2}{\partial x^2} - \mathrm{i}\omega_{kk}(X)k_0(X)\frac{\partial}{\partial x} - \left(\frac{1}{2}\omega_{kk}(X)k_0^2(X) + \omega_0(X)\right)\right]\Psi(x,t;\varepsilon) = 0, \tag{2.1}$$

where the independent variables t and x designate time and the propagation direction, respectively. To mimic the non-parallel nature of spatially developing flows, the properties of the underlying basic state are assumed to be functions of a slow space variable $X = \varepsilon x$, where ε is a small parameter characterizing the inhomogeneities of the medium. The complex analytic functions $\omega_{kk}(X)$, $k_0(X)$ and $\omega_0(X)$ appearing in (2.1) fully specify the nature of the local dispersion relation at each station X, as discussed below following equation (2.5).

The Ginzburg–Landau equation with constant coefficients is ubiquitous in numerous analytical studies of hydrodynamic instabilities close to threshold. It is also one of the simplest generic models for the study of pattern formation in nonlinear systems,

as recently reviewed by Newell *et al.* (1993). In fact, this model arises frequently in the literature on quantum mechanics (Pokrovskii & Khalatnikov 1961) to describe bound states in potential-well problems and it is well established that immersion in the complex plane is necessary to correctly handle terms that are exponentially small with respect to each other. In the present context, it can be argued that equation (2.1) displays the minimum structure necessary for the existence of a global mode on the infinite interval, namely two spatial branches $k^+(X;\omega)$ and $k^-(X;\omega)$ (see equation (2.6)). Finally, the presence of a first-order space derivative in (2.1) ensures that the local reflection symmetry $x \to -x$ has been broken, as in most open flow configurations with a dominant advection direction.

Model equation (2.1) being invariant under arbitrary time translations $t \to t +$ const., it is legitimate to seek solutions of the form

$$\Psi(x,t;\varepsilon) = \psi(X;\omega,\varepsilon)\mathrm{e}^{-\mathrm{i}\omega t}, \tag{2.2}$$

where ω is a complex frequency. The spatial distribution function $\psi(X;\omega,\varepsilon)$ is then governed by the second-order differential equation

$$\left[\omega + \frac{1}{2}\omega_{kk}(X)\frac{\partial^2}{\partial x^2} - \mathrm{i}\omega_{kk}(X)k_0(X)\frac{\partial}{\partial x} - \left(\frac{1}{2}\omega_{kk}(X)k_0^2(X) + \omega_0(X)\right)\right]\psi(X;\omega,\varepsilon) = 0. \tag{2.3}$$

The assumed time-harmonic fluctuation (2.2) defines a global mode solution if $\psi(X;\omega,\varepsilon)$ satisfies (2.3) subject to the boundary conditions

$$\lim_{X\to\pm\infty}\psi = 0. \tag{2.4}$$

This typically constitutes an eigenvalue problem whereby solutions are obtained only for specific complex eigenvalues, i.e. global frequencies ω_{g}, and associated eigenfunctions $\psi(X;\omega_{\mathrm{g}},\varepsilon)$. It is expected that, for arbitrary initial conditions, only the most unstable global mode with the largest growth rate $\omega_{\mathrm{g,i}}$ will prevail for large time. The main objective of the present study is then the prediction of the most unstable global frequency and associated spatial distribution as given from linear stability analysis.

The local dispersion relation associated with equation (2.1) is readily derived by performing the substitutions

$$\frac{\partial}{\partial x} \to \mathrm{i}k, \quad \frac{\partial}{\partial t} \to -\mathrm{i}\omega.$$

One obtains a single *temporal mode* given by

$$\omega = \omega_0(X) + \tfrac{1}{2}\omega_{kk}(X)(k - k_0(X))^2. \tag{2.5}$$

The frequency ω is seen to be a simple quadratic function of wavenumber k. The form of (2.1) in physical space simply reflects the nature of the local dispersion relation in Fourier space. Note in particular that $k = k_0(X)$ satisfies $\partial\omega/\partial k(k,X) = 0$. As shown in the next section, $k_0(X)$ is indeed the local absolute wavenumber and $\omega_0(X)$ the corresponding local absolute frequency. In order to enforce causality, we shall assume throughout that sufficiently large wavenumbers are damped, i.e. $\omega_{kk,\mathrm{i}}(X) < 0$ for all X real, and that $\omega_{kk}(X)$ is non-zero in the entire complex X plane.

As seen from (2.5), there exist for each value of the frequency ω two local *spatial*

branches given by

$$k^{\pm}(X;\omega) = k_0(X) \pm \sqrt{2\frac{\omega - \omega_0(X)}{\omega_{kk}(X)}}, \tag{2.6}$$

where it is understood that a specific choice has been made for the branch cut of the square root, for instance the principal value.

In the case of a slowly varying medium, $\varepsilon \ll 1$, it is possible to directly relate the global solutions of (2.3)–(2.4) to the local dispersion relation (2.5) by means of WKBJ approximations. It is well established (see, for example, Bender & Orszag 1978; Wasow 1985) that, at each point distinct from a turning point, the two WKBJ approximations

$$A^{\pm}(X;\omega,\varepsilon)\exp\left(\frac{\mathrm{i}}{\varepsilon}\int^{X} k^{\pm}(s;\omega)\,\mathrm{d}s\right),$$

are asymptotic representations when $\varepsilon \to 0$, of two independent solutions of (2.3). The amplitudes $A^{\pm}(X;\omega,\varepsilon)$ may be expanded in powers of ε and each successive term computed recursively. The global mode of frequency ω_{g} is then locally approximated in different regions of the complex X plane by either

$$A^{+}(X;\omega_{\mathrm{g}},\varepsilon)\exp\left(\frac{\mathrm{i}}{\varepsilon}\int^{X} k^{+}(s;\omega_{\mathrm{g}})\,\mathrm{d}s\right),$$

or

$$A^{-}(X;\omega_{\mathrm{g}},\varepsilon)\exp\left(\frac{\mathrm{i}}{\varepsilon}\int^{X} k^{-}(s;\omega_{\mathrm{g}})\,\mathrm{d}s\right).$$

We recall that a given approximation is said to be subdominant (resp. dominant) when it is exponentially small (resp. large) with respect to the other approximation. Furthermore, WKBJ approximations usually break down in the neighbourhood of turning points in the complex X plane which, for each frequency ω, are defined by the relation

$$k^{+}(X;\omega) = k^{-}(X;\omega). \tag{2.7}$$

Equivalently, according to (2.6), turning points are given, for each ω, by the roots of

$$\omega_0(X) = \omega. \tag{2.8}$$

In other words, there is a direct relationship, via the transformation $\omega \to X = \omega_0^{-1}(\omega)$, between the frequency ω and the location of the turning points in the complex X plane. The order m of a given turning point is, by definition, equal to the multiplicity of the corresponding root of (2.7) or (2.8). Thus, a simple turning point ($m = 1$) is a simple root of (2.8). Similarly a double-turning point ($m = 2$) corresponds to a double root of (2.8) such that

$$\frac{\mathrm{d}\omega_0}{\mathrm{d}X} = 0.$$

It is important to summarize some of the standard results pertaining to the behaviour of WKBJ approximations in the vicinity of turning points. The reader is referred to Bender & Orszag (1978) for a more comprehensive presentation in a general context and to Chomaz *et al.* (1991) for more details concerning the present Ginzburg–Landau model. To each turning point X_1, one may associate a specific

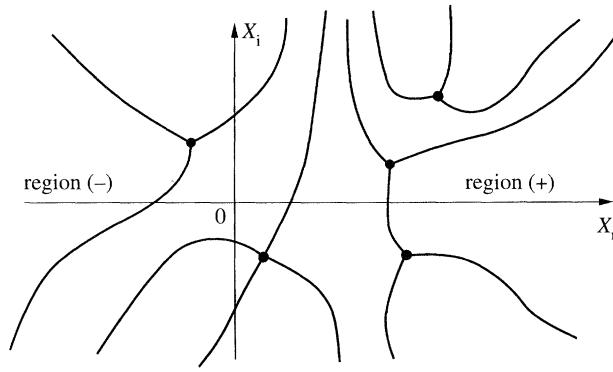

Figure 1. Illustrative sketch of typical Stokes line network.

network of Stokes lines issuing from it and defined by

$$\mathrm{Im}\left\{\int_{X_1}^{X}[k^+(s;\omega)-k^-(s;\omega)]\,\mathrm{d}s\right\}=0, \tag{2.9}$$

equivalently, according to (2.6),

$$\mathrm{Im}\left\{\int_{X_1}^{X}\sqrt{2\frac{\omega-\omega_0(s)}{\omega_{kk}(s)}}\,\mathrm{d}s\right\}=0. \tag{2.10}$$

The above definition implies that both WKBJ approximations become of equal order of magnitude on Stokes lines. In general, a given WKBJ approximation may change from subdominant to dominant or vice-versa as successive Stokes lines are crossed on a closed curve encircling the turning point X_1. It can readily be demonstrated that $(m+2)$ Stokes lines radiate from a turning point of order m, the angle between consecutive Stokes lines at X_1 being $2\pi/(m+2)$. Thus it can be concluded that turning points and Stokes lines form a network which partitions the complex X plane into sectors, as illustrated on figure 1.

It is generally impossible to obtain a uniformly valid WKBJ approximation to a solution in a domain that is larger than a single sector delimited by consecutive Stokes lines. However, there is an important exception: when a solution is asymptotic to a WKBJ approximation that is subdominant in one sector, that same approximation remains valid in the neighbouring sectors where it is then dominant (Bender & Orszag 1978; Wasow 1985). In other words, a WKBJ approximation remains valid beyond the Stokes lines defining the subdominant region. This interesting property yields necessary conditions to be satisfied by the Stokes line network of a global mode, as shown by Chomaz *et al.* (1991). These conditions are examined in the next section.

3. Necessary conditions for the existence of global modes

It is convenient to introduce a few definitions pertaining to dispersion relation (2.5). Since we have assumed $\omega_{kk,\mathrm{i}}(X)<0$ for all X real, the local temporal growth rate $\omega_{\mathrm{i}}(k;X)$ admits at each location X a finite maximum $\omega_{\mathrm{i,max}}(X)$ over all

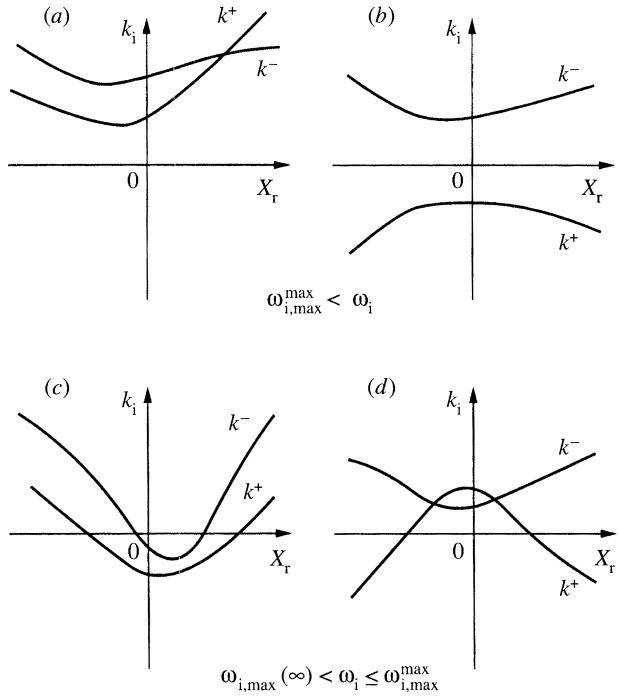

Figure 2. Imaginary part of the spatial branches $k^+(X;\omega)$ and $k^-(X;\omega)$ versus the real location X_r at a fixed complex value of ω: (a), (b), $\omega_i > \omega_{i,max}^{max}$, both branches have an imaginary part of constant sign for all X_r; (c), (d), $\omega_{i,max}(\infty) < \omega_i \leqslant \omega_{i,max}^{max}$, both branches have an imaginary part of constant sign for $|X_r|$ sufficiently large. As shown in the text, the only permissible configurations are those sketched in (b) and (d).

real wavenumbers given by

$$\omega_{i,max}(X) \equiv \max_{k \text{ real}} \omega_i(k;X) = \omega_{0,i}(X) - \frac{|\omega_{kk}(X)|^2}{2\omega_{kk,i}(X)} k_{0,i}^2(X). \tag{3.1}$$

As seen by inspection of (3.1), the local maximum growth rate $\omega_{i,max}(X)$ is necessarily larger than $\omega_{0,i}(X)$ at the same location:

$$\omega_{0,i}(X) \leqslant \omega_{i,max}(X). \tag{3.2}$$

Furthermore, let $\omega_{i,max}^{max}$ and $\omega_{0,i}^{max}$ denote the respective maxima of $\omega_{i,max}(X)$ and $\omega_{0,i}(X)$ over all X real, and $\omega_{i,max}(\infty)$ be the larger of the two limiting values taken by $\omega_{i,max}(X)$ at $X = +\infty$ and $X = -\infty$. By construction, the following inequalities hold:

$$\omega_{i,max}(\infty) \leqslant \omega_{i,max}^{max}, \quad \omega_{0,i}^{max} \leqslant \omega_{i,max}^{max}.$$

According to the above definitions, when $\omega_i > \omega_{i,max}^{max}$, there is no solution ω of the dispersion relation with k real for all X real. In other words, when $\omega_i > \omega_{i,max}^{max}$, the two spatial branches $k^+(X;\omega)$ and $k^-(X;\omega)$ cannot cross the k_r-axis for all X real (figure $2a, b$).

This necessarily means that the branches k^+ and k^- are either located on the same side of the k_r-axis (figure $2a$) or on opposite sides (figure $2b$). As ω_i decreases within the range $\omega_{i,max}(\infty) < \omega_i \leqslant \omega_{i,max}^{max}$, the relative positions of $k^+(X;\omega)$ and $k^-(X;\omega)$ with respect to the real k-axis are unchanged for $|X|$ sufficiently large,

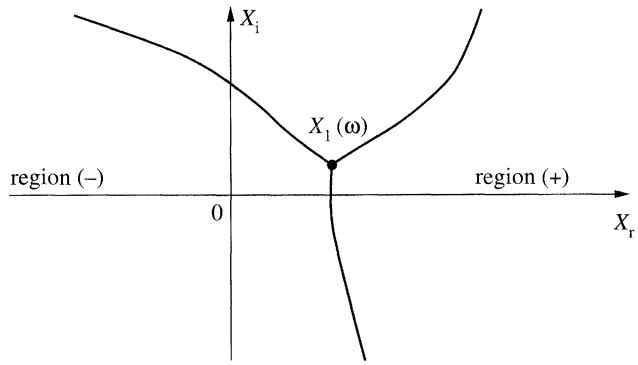

Figure 3. Stokes line network with a single first-order turning point. No global modes.

as sketched on figures 2*c*, *d*. Configurations of the type shown on figures 2*a* and *c* are clearly not admissible: both WKBJ approximations are exponentially decaying at $X = +\infty$, as required by the boundary conditions (2.4), but they grow exponentially at $X = -\infty$. It can therefore be concluded that, *in order to obtain global solutions of growth rate larger than* $\omega_{i,\max}(\infty)$, *the spatial branches* $k^+(X;\omega)$ *and* $k^-(X;\omega)$ *should necessarily be located on opposite sides of the* k_r*-axis, at least for* $|X|$ *sufficiently large*, as illustrated in figures 2*b* and *d*. Note that in such a case, $k_0(X)$ is the colliding point of both branches k^+ and k^- located on opposite sides of the k_r-axis for $\omega_i > \omega_{i,\max}(X)$: $k_0(X)$ is truly the local absolute wavenumber and $\omega_0(X) \equiv \omega(k_0(X);X)$ the corresponding local absolute frequency as defined in Bers (1983).

The above result has important consequences regarding the nature of the Stokes line network associated with equation (2.3). It implies that Stokes lines cannot be asymptotic to the X_r-axis when $\omega_i > \omega_{i,\max}(\infty)$. If they were, it would require, according to definition (2.9), that $\mathrm{Im}[k^+(X;\omega) - k^-(X;\omega)] \to 0$, as $X \to \pm\infty$, but this situation has just been excluded in the previous paragraph (see also figure 2), which proves the statement. Since Stokes lines are not asymptotic to X_r, *regions* (+) *and* (−), *delimited by Stokes lines and containing the* X_r*-axis near* $+\infty$ *and* $-\infty$ *(see figure 1), are unambiguously defined for any* $\omega_i > \omega_{i,\max}(\infty)$. Furthermore, regions (+) and (−) cannot flip from one side of a Stokes line to the other for large $|X|$ as long as $\omega_i > \omega_{i,\max}(\infty)$.

The allowable configurations of spatial branches sketched on figures 2*b*, *d* also imply the following property: when $\omega_i > \omega_{i,\max}(\infty)$, one spatial branch is necessarily amplified for sufficiently large $|X|$ along the X_r-axis while the other branch is damped, i.e. subdominant. Thus, in order to enforce the boundary conditions at infinity, *a global mode must be represented by subdominant* WKBJ *approximations in both regions* (+) *and* (−).

Since the subdominant WKBJ approximation in, say, region (−) becomes dominant as a Stokes line delimiting region (−) is crossed, we immediately deduce that *regions* (+) *and* (−) *cannot be contiguous if a global mode solution is to be obtained.* For instance, in the single first-order turning point geometry depicted on figure 3, regions (+) and (−) are always neighbours and no global modes can be found.

By contrast, when two simple turning points are present there exist Stokes line configurations that definitely cannot sustain a global mode, as in figure 4*a*, and others that may sustain one, as in figures 4*b*–*d*.

The Stokes line network evolves from one configuration to another as ω varies. We shall assume that the number of turning points (with counted multiplicity) remains

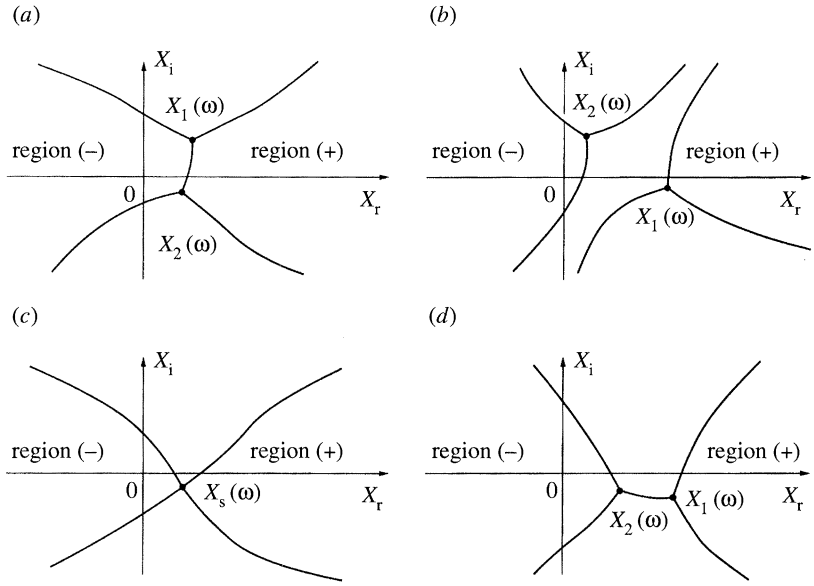

Figure 4. Typical Stokes line networks with two turning points: (*a*) two simple turning points, no global modes; (*b*) two simple turning points, global mode *a priori* possible; (*c*) one double-turning point, global mode *a priori* possible; (*d*) two simple turning points, global mode *a priori* possible.

constant in the process. The frequencies that can be excluded from consideration on the basis of the above necessary condition then constitute a set Δ_0 in the complex ω plane which can be succinctly analysed. In the case of one simple turning point, we have concluded that no global modes can be found so that Δ_0 coincides with the entire ω plane. In the case of two simple turning points $X_1(\omega)$ and $X_2(\omega)$, or one double-turning point X_s, the set Δ_0 corresponds to ω values such that a Stokes line connects $X_1(\omega)$ and $X_2(\omega)$ and separates (+) and (−) regions, as in figure 4*a*. The ensemble Δ_0 is then a subset of a larger set Δ defined by the single condition that $X_1(\omega)$ and $X_2(\omega)$ are connected by a Stokes line. For future reference, we call Δ_1 the complement of Δ_0 in Δ. The set Δ_1 corresponds to ω values such that the Stokes line network is as illustrated on figures 4*c*, *d*. According to definition (2.9) for the Stokes lines, the set Δ is defined by

$$f(\omega) \equiv \mathrm{Im}\left\{ \int_{X_1(\omega)}^{X_2(\omega)} [k^+(s;\omega) - k^-(s;\omega)]\,\mathrm{d}s \right\} = 0. \tag{3.3}$$

The vanishing of the functional $f(\omega)$ is exceptional: it generally defines Δ as a curve or set of curves in the complex ω plane. The subset Δ_0 of Δ is then even smaller. As the number of turning points increases, the dimension of Δ_0 decreases since additional conditions of type (3.3) have to be enforced. In fact, the measure of Δ_0 becomes zero as soon as the number of turning points exceeds two: the necessary condition based on the argument that (+) and (−) regions cannot be contiguous then becomes hopelessly inefficient in excluding regions of the complex ω plane as possible global frequencies.

The above reasoning solely relies on the use of *local* WKBJ approximations to represent the spatial distribution of the eigenmodes and to derive necessary existence conditions. The *global* structure of the Stokes line network in the complex X plane is not incorporated in these local approximations. Such an approach is clearly adequate

to reach a conclusion as long as the local behaviour around a single turning point provides information regarding the global behaviour of the solution for all X. This is effectively the case for the single turning point configuration of figure 3 and the two turning-point configuration of figure 4*a*. In both instances, (+) and (−) regions are connected through a single turning point and the behaviour of the solutions in each of these regions is directly related to the local WKBJ approximations around only that turning point. The necessary condition for the existence of a global mode is then identical to that of a function that must be analytic at the turning point with given local subdominant WKBJ approximations in regions (+) and (−). Such a simple reasoning fails for other configurations, such as those in figure 4*d*, when it is necessary to relate several local WKBJ approximations pertaining to distant turning points $X_1(\omega)$ and $X_2(\omega)$. The local analysis is even more problematic for general Stokes line networks of the kind displayed in figure 1 and involving many turning points.

In order to deal with distant turning-point configurations, we prefer to resort to another method based on the derivation of approximations that are uniformly valid in a much wider domain containing all turning points and associated Stokes lines between region (+) and (−). The main steps of this approach are introduced in the next section.

4. General methodology

The principle of the method of uniform approximations was first outlined by Langer (1949). Subsequent developments and refinements have been introduced by many authors including McKelvey (1955) and Lynn & Keller (1970) among others. We shall follow the general treatment of Lynn & Keller (1970) for a class of second-order differential equations with μ turning points.

Under the change of dependent variable

$$\psi(X;\omega,\varepsilon) = \phi(X;\omega,\varepsilon)\exp\left(\frac{\mathrm{i}}{\varepsilon}\int_{X_0}^{X} k_0(s)\,\mathrm{d}s\right), \quad X_0 \text{ arbitrary constant}, \tag{4.1}$$

equation (2.3) is transformed into the normalized equation for ϕ:

$$\varepsilon^2\frac{\partial^2\phi}{\partial X^2} + (R_0(X;\omega) + \varepsilon R_1(X))\phi = 0, \tag{4.2}$$

where the varying coefficients $R_0(X;\omega)$ and $R_1(X)$, introduced by Lynn & Keller (1970), take the particular form

$$R_0(X;\omega) = [k^+(X;\omega) - k^-(X;\omega)]^2 = 2\frac{\omega-\omega_0(X)}{\omega_{kk}(X)}, \tag{4.3a}$$

$$R_1(X) = \mathrm{i}k_{0X}(X). \tag{4.3b}$$

A uniform approximation to the solutions of (4.2) is given by equation (LK 1.3) of Lynn & Keller (1970). In terms of the original dependent variable ψ, this uniform approximation reduces to

$$\psi(X;\omega,\varepsilon) = \left\{B(X;\omega,\varepsilon)V\left[\frac{\eta(X;\omega)}{\varepsilon^{2/(\mu+2)}}\right] + \varepsilon^{\mu/(\mu+2)}C(X;\omega,\varepsilon)V'\left[\frac{\eta(X;\omega)}{\varepsilon^{2/(\mu+2)}}\right]\right\} \times \exp\left(\frac{\mathrm{i}}{\varepsilon}\int_{X_0}^{X} k_0(s)\,\mathrm{d}s\right). \tag{4.4}$$

The functions $B(X;\omega,\varepsilon)$ and $C(X;\omega,\varepsilon)$ admit the following expansions in powers of ε, as $\varepsilon \to 0$:

$$B(X;\omega,\varepsilon) = \sum_{l=0}^{\infty} B_l(X;\omega)\varepsilon^l, \tag{4.5a}$$

$$C(X;\omega,\varepsilon) = \sum_{l=0}^{\infty} C_l(X;\omega)\varepsilon^l. \tag{4.5b}$$

Turning points of (4.2) correspond to zeros of $R_0(X;\omega)$ given by (4.3 *a*), i.e. to roots of (2.7) or equivalently (2.8), as discussed in § 2.

When μ turning points with counted multiplicity are present, the function $V(\xi)$ appearing in (4.4) satisfies the so-called comparison equation

$$V''(\xi) + \left(\sum_{m=0}^{\mu} \gamma_m(\omega,\varepsilon)\xi^m\right) V(\xi) = 0, \tag{4.6}$$

where the $(\mu+1)$ coefficients $\gamma_m(\omega,\varepsilon)$ admit expansions in powers of ε given by

$$\gamma_m(\omega,\varepsilon) = \varepsilon^{2(m-\mu)/(\mu+2)} \sum_{p=0}^{\infty} \gamma_{m_p}(\omega)\varepsilon^p. \tag{4.7}$$

Note that only two of the parameters γ_m, for instance $\gamma_1(\omega,\varepsilon)$ and $\gamma_2(\omega,\varepsilon)$, can be assigned arbitrary values. All other γ_m are then linear combinations of γ_1 and γ_2.

The conformal mapping

$$X \mapsto \eta(X;\omega)/\varepsilon^{2/(\mu+2)} \tag{4.8}$$

is chosen so as to transform the normalized equation (4.2) into the comparison equation (4.6) at leading order in ε. It is found to satisfy

$$\int_{\eta_0}^{\eta(X;\omega)} \sqrt{\sum_{m=0}^{\mu} \gamma_{m_0}(\omega)s^m}\,\mathrm{d}s = \int_{X_0}^{X} \sqrt{R_0(r;\omega)}\,\mathrm{d}r, \tag{4.9}$$

where the arbitrarily chosen constant η_0 defines the image of X_0 under the mapping. Once the $\mu+1$ coefficients $\gamma_{m_0}(\omega)$ have been determined, the above equation implicitly defines the change of independent variable $X \mapsto \eta(X;\omega)$. Note that, according to (4.9), turning points of the original equation (4.2), given by $R_0(X;\omega) = 0$, equivalently $\omega_0(X) = \omega$, are mapped into turning points of comparison equation (4.6), given by $\sum_{m=0}^{\mu} \gamma_{m_0}(\omega)\eta^m = 0$. Furthermore, Stokes line networks issuing from each turning point in the X plane are mapped into Stokes line networks of the corresponding image turning point in the η plane. The branches of the square roots appearing in (4.9) may be specified arbitrarily, provided that the branch cuts of the right- and left-hand side square roots are mapped onto each other.

The reader is referred to Lynn & Keller (1970) for a comprehensive discussion of the recursive algorithm leading to the determination of the coefficients $\gamma_{m_p}(\omega)$ and the functions $B_l(X;\omega)$ and $C_l(X;\omega)$. In the present study, we are only interested in turning points that directly influence the structure of the global mode on the real line, i.e. those with Stokes lines crossing the X_r-axis. In this case, approximation (4.4) is known to be uniformly valid in a domain of the complex X plane containing these μ turning points.

There remains to specify the eigenvalue problem to be solved in the transformed

η plane. Boundary conditions on $V[\eta(X;\omega)/\varepsilon^{2/(\mu+2)}]$ have to be applied in regions $\eta(+;\omega)$ and $\eta(-;\omega)$, which are the images of regions (+) and (−) under the mapping $X \mapsto \eta(X;\omega)$. The properties of WKBJ approximations near infinity derived in § 3 can be transposed from the X plane into the η plane. Recall first that, among the two branches $k^+(X;\omega)$ and $k^-(X;\omega)$ defined in (2.6), one must necessarily have a positive imaginary part and the other a negative one as $X \to \pm\infty$. In view of relation (4.3 *a*), $\operatorname{Im}\sqrt{R_0(X;\omega)} = \operatorname{Im}[k^+(X;\omega) - k^-(X;\omega)]$, and this behaviour implies that $\operatorname{Im}\sqrt{R_0(X;\omega)}$ does not tend to zero as $X \to \pm\infty$. Consequently, the integral on the right-hand side of (4.9) is necessarily divergent when $X \to \pm\infty$, which guarantees that $|\eta(X;\omega)| \to \infty$ as $X \to \pm\infty$. Thus, *points at infinity in the* (+) *and* (−) *regions are mapped into points at infinity in the* $\eta(+;\omega)$ *and* $\eta(-;\omega)$ *regions.*

According to the form of equation (4.6), two independent solutions $V(\xi)$ can be chosen to be exponentially increasing and decreasing, respectively, near infinity in the $\eta(+;\omega)$ and $\eta(-;\omega)$ regions. When such solutions are substituted into approximation (4.4), they necessarily give rise to amplified and decaying solutions, respectively, near $X = \infty$, since the WKBJ approximations of ψ do exhibit this behaviour. It follows that the exponential factor $\exp\{(\mathrm{i}/\varepsilon)\int_{X_0}^{X} k_0(s)\,\mathrm{d}s\}$ and the functions $B(X;\omega,\varepsilon)$ and $C(X;\omega,\varepsilon)$ do not alter the growing or decaying nature of the solutions near infinity. It can therefore be concluded that the original eigenvalue problem is mapped into a new eigenvalue problem in the η plane whereby $V(\xi)$ *should satisfy comparison equation (4.6) and be exponentially small in regions* $\eta(+;\omega)$ *and* $\eta(-;\omega)$ *as* $|\eta| \to \infty$. This is a necessary and sufficient condition for the existence of global modes.

It should be stressed that global modes on the real X-axis do not automatically map into eigenfunctions of the comparison equation for V on the *real* η-axis. The regions $\eta(+;\omega)$ and $\eta(-;\omega)$ do not always contain the real η-axis as $|\eta|$ tends to infinity. It is therefore essential to accurately locate the $\eta(+;\omega)$ and $\eta(-;\omega)$ domains before proceeding to a formal solution of the problem. Otherwise incorrect results might be obtained (see § 5 *b* for details).

It is generally difficult to implement the method of uniform approximations when more than two turning points are involved. The solutions of the comparison equation (4.6) are then not well documented although some partial results have been derived in particular situations (Sibuya 1975). In the next section, the above formulation is applied to the determination of all global modes when two turning points with counted multiplicity (two simple turning points or one double-turning point) are present.

5. Global modes with two turning points

It is assumed that only two simple turning points $X_1(\omega)$ and $X_2(\omega)$, possibly degenerating into a single double-turning point at X_s, are involved in the selection of global mode frequencies.

(*a*) *Mapping and comparison equation*

When $\mu = 2$, the formal solution (4.4) reduces to

$$\psi(X;\omega,\varepsilon) = \left\{ B(X;\omega,\varepsilon)V\left[\frac{\eta(X;\omega)}{\sqrt{\varepsilon}}\right] + \sqrt{\varepsilon}C(X;\omega,\varepsilon)V'\left[\frac{\eta(X;\omega)}{\sqrt{\varepsilon}}\right]\right\} \times \exp\left(\frac{\mathrm{i}}{\varepsilon}\int_{X_0}^{X} k_0(s)\,\mathrm{d}s\right). \tag{5.1}$$

PHILOSOPHICAL TRANSACTIONS OF THE ROYAL SOCIETY A MATHEMATICAL, PHYSICAL & ENGINEERING SCIENCES

When $\mu = 2$, comparison equation (4.6) involves only three coefficients γ_0, γ_1 and γ_2, only one of which is independent. According to Lynn & Keller (1970), one may, without loss of generality, set $\gamma_1(\omega, \varepsilon) = 0$ and $\gamma_2(\omega, \varepsilon) = -\frac{1}{4}$, the only unknown parameter being $\gamma_0(\omega, \varepsilon)$. Equation (4.6) therefore reduces to

$$V''(\xi) + [\gamma_0(\omega, \varepsilon) - \tfrac{1}{4}\xi^2]V(\xi) = 0. \tag{5.2}$$

As in (4.7), the coefficient $\gamma_0(\omega, \varepsilon)$ can be expanded in powers of ε to read

$$\gamma_0(\omega, \varepsilon) = \varepsilon^{-1} \sum_{p=0}^{\infty} \gamma_{0_p}(\omega)\varepsilon^p. \tag{5.3}$$

It is convenient to express the leading-order approximation $\gamma_{0_0}(\omega)$ in terms of a new parameter $\eta_1(\omega)$ such that

$$\gamma_{0_0}(\omega) \equiv \tfrac{1}{4}\eta_1^2(\omega). \tag{5.4}$$

Equation (5.2), together with exponential decay conditions at infinity in the $\eta(+;\omega)$ and $\eta(-;\omega)$ regions, defines the new eigenvalue problem in the complex η plane in terms of the unknown eigenvalues $\gamma_0(\omega, \varepsilon)$ and unknown eigenfunctions $V(\xi)$.

In view of the above expressions for $\gamma_{0_0}(\omega)$, $\gamma_1(\omega, \varepsilon)$ and $\gamma_2(\omega, \varepsilon)$, and definition (4.3 *a*) for $R_0(X;\omega)$, relation (4.9) reduces to

$$\int_{\eta_0}^{\eta(X;\omega)} \sqrt{\eta_1^2(\omega) - s^2}\, \mathrm{d}s = 2\int_{X_0}^{X} \sqrt{2\frac{\omega - \omega_0(r)}{\omega_{kk}(r)}}\, \mathrm{d}r. \tag{5.5}$$

This relation implicitly defines the mapping $X \mapsto \eta(X;\omega)$ for each value of ω. As stated in the previous section, the turning points $X_1(\omega)$ and $X_2(\omega)$, which satisfy $\omega_0(X) = \omega$, should be transformed into turning points $\eta_1(\omega)$ and $-\eta_1(\omega)$ of comparison equation (5.2). Consequently, if one chooses $\eta_1(\omega) = \eta[X_1(\omega);\omega]$, one should also have $-\eta_1(\omega) = \eta[X_2(\omega);\omega]$. According to (5.5), these relations imply that

$$\int_{\eta_1(\omega)}^{-\eta_1(\omega)} \sqrt{\eta_1^2(\omega) - s^2}\, \mathrm{d}s = 2\int_{X_1(\omega)}^{X_2(\omega)} \sqrt{2\frac{\omega - \omega_0(X)}{\omega_{kk}(X)}}\, \mathrm{d}X. \tag{5.6}$$

This identity remains valid when the right-hand side integral is evaluated along any path Γ joining both turning points $X_1(\omega)$ and $X_2(\omega)$, provided that the image path $\eta(\Gamma;\omega)$ is chosen to calculate the left-hand side integral. When a specific choice of branch is made for the square root on the left-hand side, the integral can readily be calculated to yield

$$\eta_1(\omega) = 2\left\{\frac{1}{\pi}\int_{X_1(\omega)}^{X_2(\omega)} \sqrt{2\frac{\omega - \omega_0(X)}{\omega_{kk}(X)}}\, \mathrm{d}X\right\}^{1/2}. \tag{5.7}$$

It is possible to obtain a more convenient expression for $\eta_1(\omega)$ that is independent of the labelling of the turning points $X_1(\omega)$ and $X_2(\omega)$. The branch points of the square root in (5.7) satisfy $\omega_0(X) = \omega$ and therefore coincide with the turning points $X_1(\omega)$ and $X_2(\omega)$. If the branch cut is chosen to lie between $X_1(\omega)$ and $X_2(\omega)$, equation (5.7) can also be written as

$$\eta_1(\omega) = 2\left\{\frac{1}{2\pi}\oint_C \sqrt{2\frac{\omega - \omega_0(X)}{\omega_{kk}(X)}}\, \mathrm{d}X\right\}^{1/2}, \tag{5.8}$$

where the contour C encircles both turning points. As soon as the orientation of the contour is fixed, for instance counterclockwise, the definition of $\eta_1(\omega)$ only depends on the selected branch of the square roots. Four determinations of $\eta_1(\omega)$ are possible, which can be deduced from each other by successive multiplications† by $\mathrm{e}^{\mathrm{i}k\pi/2}$, $k = 1, 2, 3$. It is only the constraint $\eta[X_1(\omega); \omega] = \eta_1(\omega)$ which allows one to obtain a unique representation of $\eta(X; \omega)$ from equation (5.5). The uniform approximation (5.1) must remain invariant when we change from one determination for $\eta_1(\omega)$ to another. Thus, one should respect the following substitutions:

$$\left|\begin{array}{lcl} \eta_1(\omega) & \mapsto & \mathrm{e}^{\mathrm{i}k\pi/2}\eta_1(\omega), \\ \eta(X;\omega) & \mapsto & \mathrm{e}^{\mathrm{i}k\pi/2}\eta(X;\omega), \\ \gamma_0(\omega,\varepsilon) & \mapsto & \mathrm{e}^{\mathrm{i}k\pi}\gamma_0(\omega,\varepsilon). \end{array}\right. \tag{5.9}$$

According to expressions (A 3 a, b) listed in Appendix A, the functions $B(X; \omega, \varepsilon)$ and $C(X; \omega, \varepsilon)$ are both multiplied by the same constant factor under the above substitutions. Without loss of generality, this factor may be taken equal to unity.

The Stokes lines in the complex η plane can explicitly be obtained from the analytical form

$$\frac{1}{4\varepsilon}[\eta_1^2(\omega) - \eta^2]$$

of the leading-order coefficient multiplying $V(\xi)$ in comparison equation (5.2). Stokes lines issuing from each turning point $\eta_1(\omega)$ and $-\eta_1(\omega)$ are, respectively, given by

$$\mathrm{Im}\left\{\int_{\pm\eta_1(\omega)}^{\eta} \sqrt{\eta_1^2(\omega) - s^2}\,\mathrm{d}s\right\} = 0. \tag{5.10}$$

Among the four possible determinations of $\eta_1(\omega)$ solutions of (5.8), one is bound to lie in the quarter plane $\frac{3}{2}\pi < \arg\eta \leqslant 2\pi$. When $\eta_1(\omega)$ is restricted in this manner, Stokes lines may take one of the three characteristic configurations represented on figure 5.

The configuration with distinct Stokes line networks for each turning point (figure 5a) is generic. Configurations with one Stokes line joining both turning points (figure 5b) or with one double-turning point (figure 5c) are exceptional. The Stokes line networks pertaining to determinations of $\eta_1(\omega)$ falling in the other three quadrants of the complex η plane may be generated by simple rotations of angle $\frac{1}{2}k\pi$, $k = 1, 2, 3$. It should be emphasized that the Stokes line network in the complex η plane is solely a function of the single complex parameter $\eta_1(\omega)$ defined in (5.8), as seen from the Stokes line equation (5.10). Recall also that Stokes lines in the complex X plane and η plane are mapped into each other when $\eta(X; \omega)$ is a solution of (5.5).

In order to completely define the eigenvalue problem in the complex η plane, there remains to locate the $\eta(+; \omega)$ and $\eta(-; \omega)$ regions where exponential decay boundary conditions at infinity have to be applied. This issue is examined in the next subsection.

† Note that the branch of

$$\sqrt{2\frac{\omega - \omega_0(X)}{\omega_{kk}(X)}}$$

in (5.8) is not necessarily the same as on the right-hand side of (5.5). The branch may change from one equation to the other depending on specific features of the mapping $X \mapsto \eta(X; \omega)$, which may or may not conserve sense of rotation.

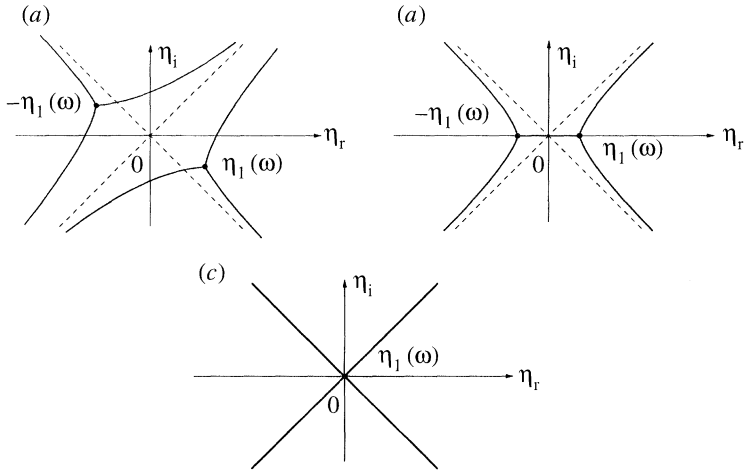

Figure 5. Possible Stokes line networks with two turning points in the complex η plane. The parameter $\eta_1(\omega)$ is restricted to lie in the quarter plane $\frac{3}{2}\pi < \arg\eta \leqslant 2\pi$: (*a*) generic configuration, no common Stokes line joins both turning points; (*b*) $\eta_1(\omega)$ on positive η_r-axis, Stokes line joins both turning points; (*c*) $\eta_1(\omega) = 0$, double-turning point. Other configurations are generated by rotations of angle $\frac{1}{2}k\pi$, $k = 1, 2, 3$.

(*b*) *'Dynamics' of the* $\eta(+;\omega)$ *and* $\eta(-;\omega)$ *regions*

It has been argued in § 3 that regions (+) and (−) containing the X_r-axis near $+\infty$ and $-\infty$ are well defined and cannot flip from one side of a Stokes line to the other as long as ω is maintained within the domain $\omega_i > \omega_{i,\max}(\infty)$. This property is preserved under the conformal transformation $X \mapsto \eta(X;\omega)$: the relative positions of $\eta(+;\omega)$ and $\eta(-;\omega)$ in the complex η plane do not change when $\omega_i > \omega_{i,\max}(\infty)$. More specifically, variations of ω should lead, in the present context, to displacements of $\eta_1(\omega)$ within the specified quarter plane $\frac{3}{2}\pi < \arg\eta \leqslant 2\pi$. If $\eta_1(\omega)$ happens to cross one of the boundary lines $\arg\eta = \frac{3}{2}\pi$ or $\arg\eta = 2\pi$, a rotation of angle $\frac{1}{2}k\pi$ must be applied to keep $\eta_1(\omega)$ within the prescribed quadrant, and $\eta(X;\omega)$ should be changed according to the rules defined in (5.9). This results in an abrupt rotation of the whole Stokes line network in the complex η plane which nonetheless preserves the relative positions of $\eta(+;\omega)$ and $\eta(-;\omega)$.

It is now possible to add on the Stokes line networks sketched on figure 5 all possible configurations taken by the regions $\eta(+;\omega)$ and $\eta(-;\omega)$. According to the comments following lemma 2 in Chomaz *et al.* (1991), the real axis crosses a single Stokes line connected to each turning point when $\omega_i > \omega_{0,i}^{\max}$ only once. Thus, when $\omega_i > \omega_{0,i}^{\max}$, permissible configurations (+) and (−) regions in the complex X plane are as sketched on figure 6. Note in particular that for $\omega_i > \omega_{0,i}^{\max}$, configurations of the form sketched on figures 4*c* and *d*, where the real axis crosses two connected Stokes lines cannot exist, although they may arise for lower values of ω_i as seen below. Possible locations of the corresponding regions $\eta(+;\omega)$ and $\eta(-;\omega)$ in the complex η plane are listed on figure 7. Note that on all configurations shown on figures 7*c*, *d*, $\eta(+;\omega)$ and $\eta(-;\omega)$ are contiguous regions in the limit of large $|\eta|$. This feature, initially valid for $\omega_i > \omega_{0,i}^{\max}$, persists for all $\omega_i > \omega_{i,\max}(\infty)$ and a solution of comparison equation (5.2) that is initially subdominant in $\eta(+;\omega)$ will become dominant in $\eta(-;\omega)$. Consequently, comparison equation (5.2) has no eigenfunctions satisfying the required boundary conditions. It can be concluded that *configurations of the* η

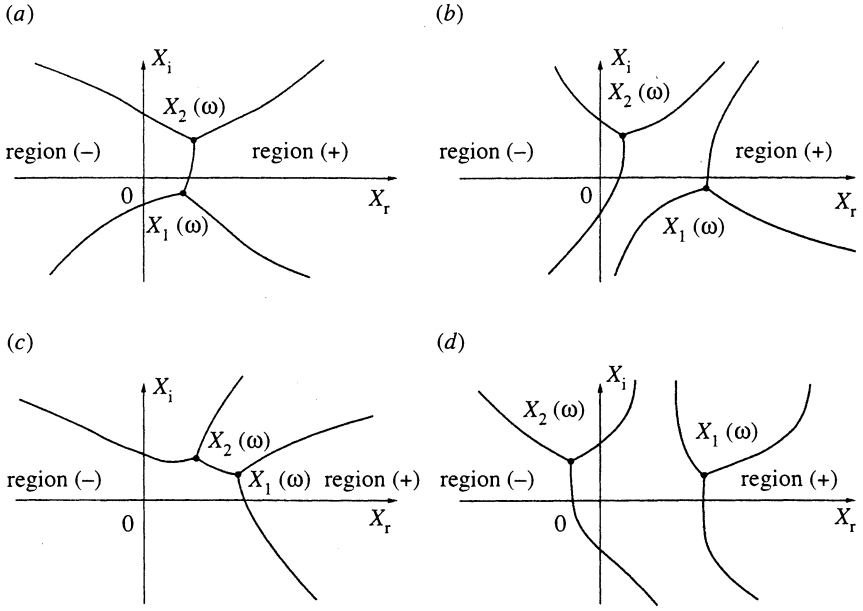

Figure 6. Stokes line networks in the complex X plane when $\omega_i \geqslant \omega_{0,i}^{max}$. ($a$) and ($b$) may potentially evolve into global mode configurations with varying ω while (c) and (d) never do.

plane shown on figure 7c, d, together with their preimages in the X plane sketched on figures 6c, d, do not correspond to global frequencies and never evolve to global mode configurations as ω *varies in the range* $\omega_i > \omega_{i,max}(\infty)$. By contrast, in the two cases described on figures 7*a*, *b*, regions $\eta(+;\omega)$ and $\eta(-;\omega)$ are not contiguous for large $|\eta|$ and they will remain so as long as $\omega_i > \omega_{i,max}(\infty)$. Preimage configurations in the X plane illustrated on figures 6*a*, *b* may therefore evolve as ω varies to give rise to global modes.

(*c*) *General global mode solutions*

It has proved convenient until now to restrict $\eta_1(\omega)$ to a particular quadrant of the complex η plane in order to identify all possible configurations of the Stokes line network and associated regions $\eta(+;\omega)$ and $\eta(-;\omega)$. This convention has led us to exclude some configurations but it is ill-fitted to effectively solve the eigenvalue problem pertaining to comparison equation (5.2). As observed in § 5 *b*, the Stokes line network, as well as regions $\eta(+;\omega)$ and $\eta(-;\omega)$, evolve discontinuously with respect to ω as $\eta_1(\omega)$ reaches the quarterplane boundaries. In the following analysis, $\eta_1(\omega)$ is no longer confined to a particular sector but it is selected so that $\eta(+;\omega)$ contains† the real η-axis for large η.

In contrast with the situation prevailing in § 5 *b*, the determination $\eta(X;\omega)$ of the mapping remains unchanged and the Stokes line network then evolves continuously

† Note that it is always possible to do so. The region $\eta(+;\omega)$ has been shown in the previous subsection never to coincide with, say, the central domain S_0 between both turning points indicated on figures 7*b*, *d*. Hence, the preimage configuration displayed on figure 8 has already been excluded. Furthermore, if $\eta(+;\omega)$ does not initially contain the η_r-axis for large η, a rotation of appropriate angle $\frac{1}{2}k\pi$ will correct the situation.

PHILOSOPHICAL TRANSACTIONS OF THE ROYAL SOCIETY A MATHEMATICAL, PHYSICAL & ENGINEERING SCIENCES

as ω varies in the domain $\omega_{\rm i} > \omega_{\rm i,max}(\infty)$. Finally, the eigenvalue $\gamma_0(\omega,\varepsilon)$ appearing in the comparison equation also stays continuous with respect to ω.

Recall that the only remaining configurations in the complex X plane which may evolve into global modes with varying ω are those illustrated on figures 6*a*, *b*. Following the procedure just outlined above, the regions $\eta(+;\omega)$ and $\eta(-;\omega)$ are always taken to correspond asymptotically for large $|\eta|$ to the sectors

$$\eta(+;\omega) : -\tfrac{1}{4}\pi < \arg\eta < \tfrac{1}{4}\pi; \tag{5.11a}$$

$$\eta(-;\omega) : \tfrac{3}{4}\pi < \arg\eta < \tfrac{5}{4}\pi. \tag{5.11b}$$

Exponential decay conditions at infinity are always enforced within these sectors as long as $\omega_{\rm i} > \omega_{\rm i,max}(\infty)$. Solutions of comparison equation (5.2), that are exponentially small in both regions $\eta(+;\omega)$ and $\eta(-;\omega)$, are expressible in terms of Hermite polynomials of order n as follows:

$$V_n(\xi) = {\rm He}_n(\xi){\rm e}^{-\xi^2/4}, \tag{5.12}$$

and corresponding eigenvalues are given by

$$\gamma_0[\omega_{{\rm g}_n}(\varepsilon),\varepsilon] = n + \tfrac{1}{2}. \tag{5.13}$$

Any function $\omega_{{\rm g}_n}(\varepsilon)$ satisfying the above functional relationship is a global frequency of the problem. Of primary interest is the derivation of a systematic approximation scheme for $\omega_{{\rm g}_n}(\varepsilon)$ in the regime $\varepsilon \ll 1$. In the sequel, it is assumed that $\omega_{{\rm g}_n}(\varepsilon)$ reaches a well defined limit $\omega_{{\rm g}_n}^{(0)}$ as $\varepsilon \to 0$. According to expansion (5.3) and definition (5.4), the leading-order approximation to $\gamma_0[\omega_{{\rm g}_n}(\varepsilon),\varepsilon]$ is then

$$\gamma_0[\omega_{{\rm g}_n}(\varepsilon),\varepsilon] = \frac{\gamma_{0_0}(\omega_{{\rm g}_n}^{(0)})}{\varepsilon} + O(1) = \frac{\eta_1^2(\omega_{{\rm g}_n}^{(0)})}{4\varepsilon} + O(1). \tag{5.14}$$

In order for these estimates to be consistent with eigenvalue relation (5.13), the integers n should be chosen such that $n(\varepsilon) = O(1/\varepsilon)$ in the limit $\varepsilon \to 0$, i.e. $n(\varepsilon)$ should satisfy

$$\lim_{\varepsilon\to 0} \varepsilon n(\varepsilon) = m, \tag{5.15}$$

with the real number m given by

$$\gamma_{0_0}(\omega_{{\rm g}_n}^{(0)}) = \tfrac{1}{4}\eta_1^2(\omega_{{\rm g}_n}^{(0)}) = m, \quad m \geqslant 0. \tag{5.16}$$

Note that the function $\eta_1(\omega)$ has explicitly been defined in (5.8).

Higher order approximations to the global frequencies $\omega_{{\rm g}_n}(\varepsilon)$ can be sought in the form

$$\omega_{{\rm g}_n} = \omega_{{\rm g}_n}^{(0)} + \varepsilon\omega_{{\rm g}_n}^{(1)} + \cdots. \tag{5.17}$$

Upon substitution into the eigenvalue relation (5.13) and identification of terms of order unity, one obtains the equation for the first-order correction $\omega_{{\rm g}_n}^{(1)}$:

$$\frac{\partial\gamma_{0_0}}{\partial\omega}(\omega_{{\rm g}_n}^{(0)})\omega_{{\rm g}_n}^{(1)} + \gamma_{0_1}(\omega_{{\rm g}_n}^{(0)}) = [n + \tfrac{1}{2} - m/\varepsilon], \tag{5.18}$$

where the first-order term $\gamma_{0_1}(\omega_{{\rm g}_n}^{(0)})$ is explicitly given in (A 1) and (A 2) of Appendix A. Relation (5.18) is valid as long as $n + \frac{1}{2} - m/\varepsilon = O(1)$ and

$$\frac{\partial\gamma_{0_0}}{\partial\omega}(\omega_{{\rm g}_n}^{(0)}) \neq 0.$$

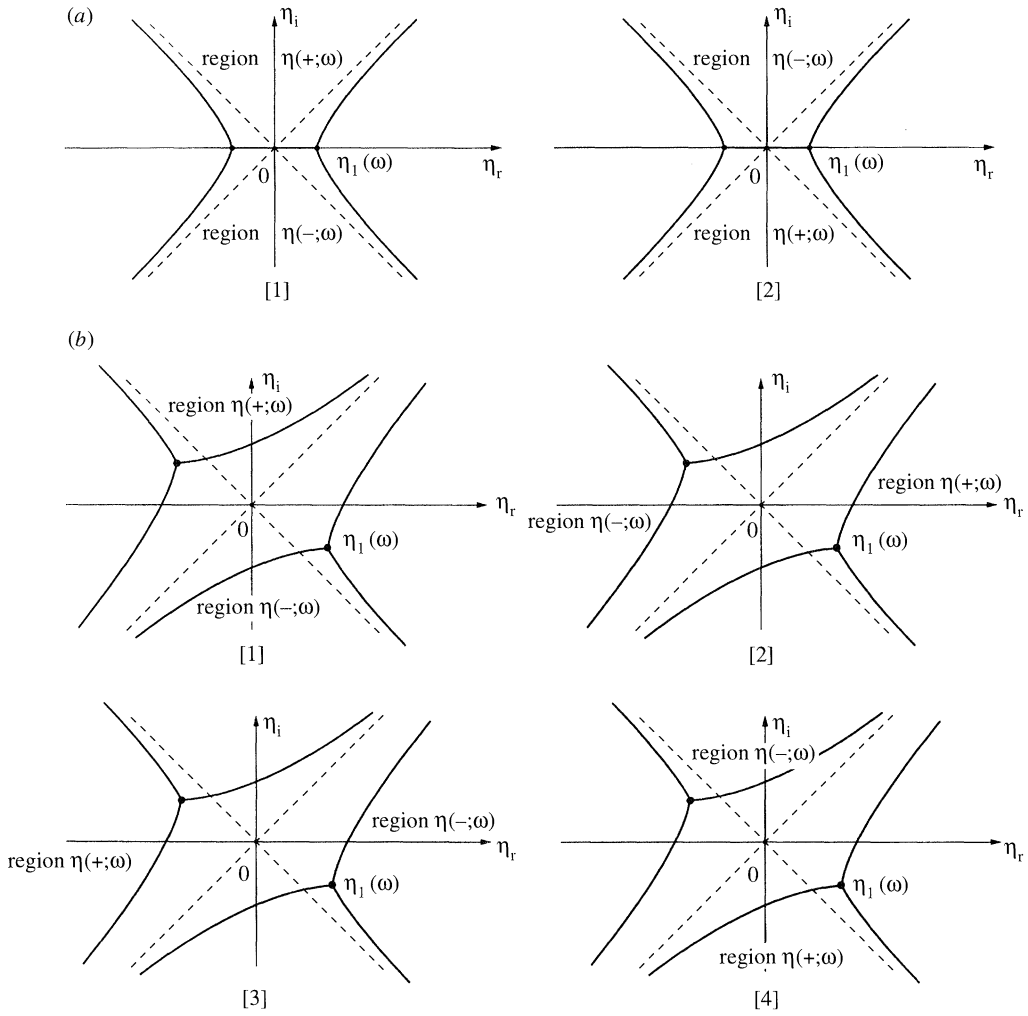

Figure 7. Stokes line networks in the complex η plane when $\omega_{\rm i} \geqslant \omega_{0,\rm i}^{\max}$. ($a$) and ($b$) may potentially evolve into global mode configurations with varying ω while (c) and (d) never do.

The procedure can readily be extended to arbitrary order to generate the entire expansion (5.17).

To the leading-order global frequencies $\omega_{{\rm g}_n}^{(0)}$ correspond specific Stokes line configurations. According to eigenvalue relation (5.16), allowable parameter values $\eta_1(\omega_{{\rm g}_n}^{(0)})$ are necessarily real and the Stokes line network in the complex η plane has one of the configurations displayed on figures 9a, b. Since the conformal mapping $X \mapsto \eta(X;\omega_{{\rm g}_n}^{(0)})$ is one to one, corresponding Stokes lines in the complex X plane are easily identified, as sketched in figures 10a, b. Figure 9a pertains to strictly positive values of m in (5.16). Such Stokes line configurations with *two simple turning points in the complex plane* are referred to as *type-1*. The eigenvalue $\omega_{{\rm g}_n}^{(0)}$ is such that the two turning points in the η plane are located at $\pm\eta_1(\omega_{{\rm g}_n}^{(0)}) = \pm 2\sqrt{m}$ on the real η-axis, as in figure 9a. Note that regions $\eta(+;\omega)$ and $\eta(-;\omega)$, as well as their preimages (+) and (−), are necessarily not contiguous, in agreement with the necessary condition stated in § 3. When $m = 0$, the Stokes line network displays *a double-turning*

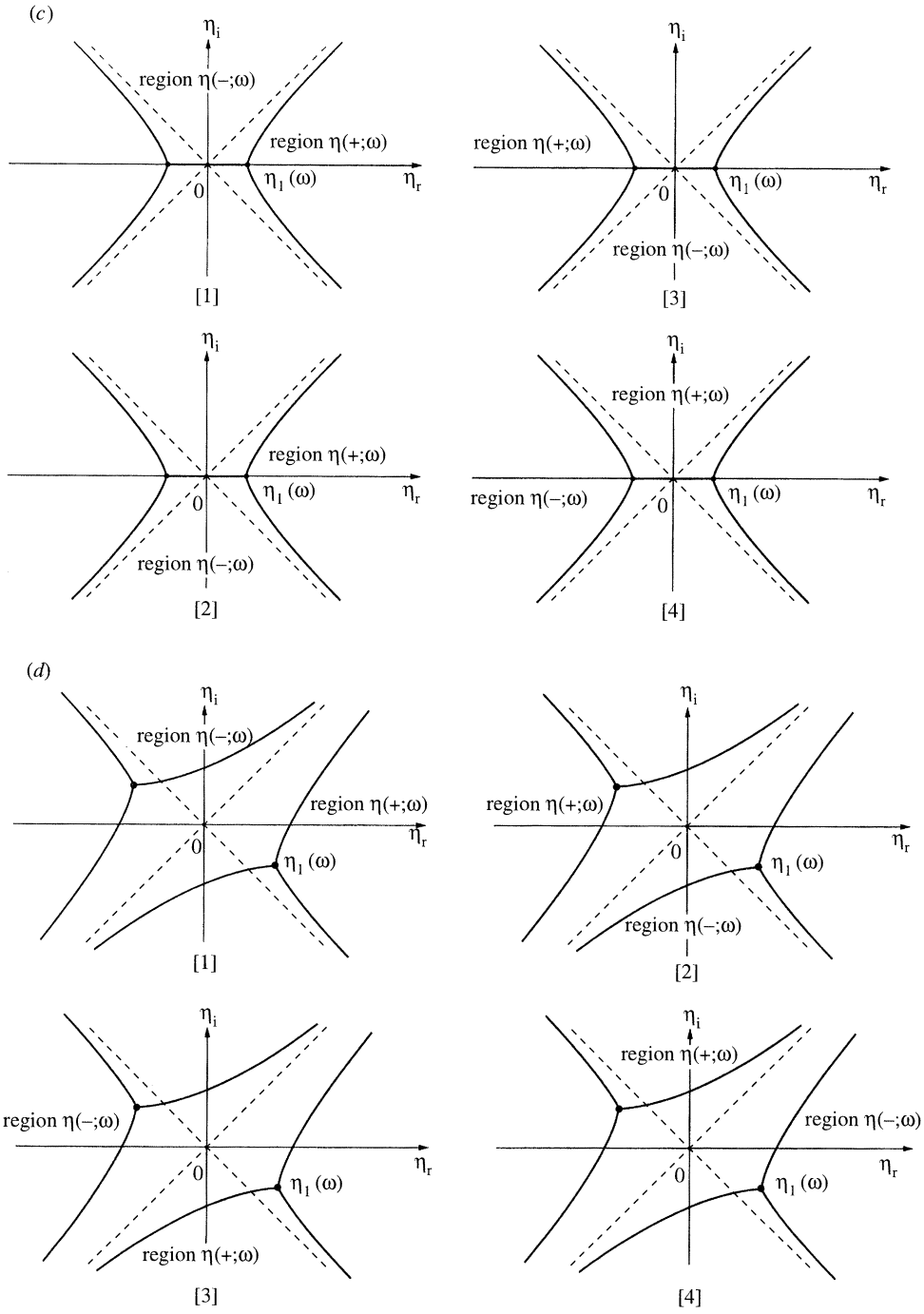

Figure 7. *Cont.*

point X_s in the complex X plane, a situation referred to as *type-2* and illustrated on figure 10*b*. The image network has also a double-turning point at the origin in the η plane, as shown on figure 9*b*. It has therefore been demonstrated that, if $\omega_{g_n}^{(0)}$ is a

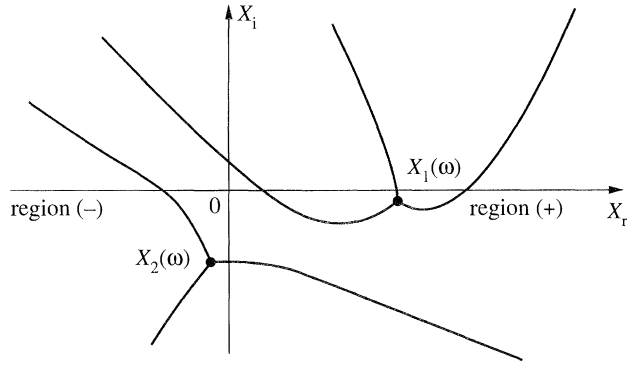

Figure 8. Example of Stokes line network in the complex X plane such that $\eta(+;\omega)$ coincides with S_0 of figures $7b, d$.

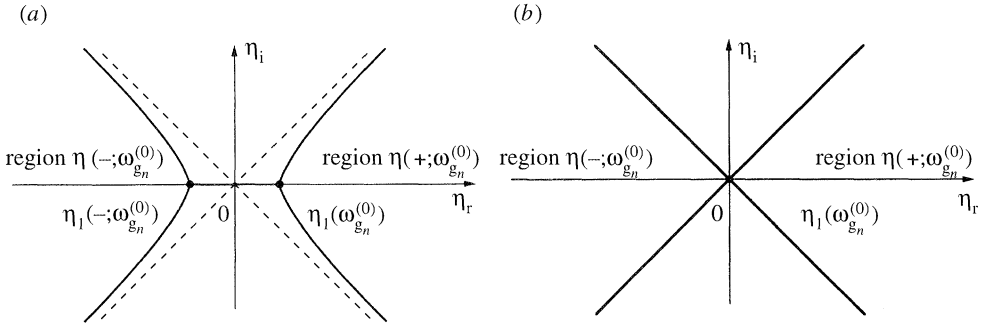

Figure 9. Stokes line networks in the complex η plane giving rise to global frequencies satisfying (5.16): (5.19): (a), $m > 0$, two simple turning points located at $\pm\eta_1(\omega_{g_n}^{(0)}) = \pm 2\sqrt{m}$ ($\eta_1(\omega_{g_n}^{(0)})$ chosen non-negative on the figure); (b), $m = 0$, one double-turning point at the origin.

global frequency, the Stokes line network in the X plane is either type-1 or type-2, as indicated in figures $10a, b$.

The reverse proposition is also true: if, for a given value $\omega^{(0)}$, the Stokes line network is either of type-1 or type-2, $\omega^{(0)}$ is, at leading order in ε, a global frequency of the problem. To prove this statement, we simply note that, if one of the configurations depicted in figures $10a, b$ prevails in the X plane for a given frequency $\omega^{(0)}$, the transformation $X \mapsto \eta(X;\omega^{(0)})$ can be selected so as to map $(+)$ into $\eta(+;\omega^{(0)})$ containing the real η-axis. The original Stokes lines in the X plane are then necessarily transformed into one of the Stokes line networks in the complex η plane shown on figures $9a, b$. Such situations are known to give rise to eigenvalues with leading-order approximation $\omega^{(0)}$. Successive terms in the expansion (5.3) of the function $\gamma_0(\omega^{(0)}, \varepsilon)$ can be evaluated. For instance, the leading-order term $\gamma_{0_0}(\omega^{(0)})$ is calculated with the help of (5.4) and (5.8). Higher order corrections $\gamma_{0_1}(\omega^{(0)}), \ldots$ are given by expressions such as (A 1) or (A 2) in Appendix A. Thus, higher order contributions to the global frequency expansion $\omega_{g_n}(\varepsilon) = \omega^{(0)} + \varepsilon\omega_{g_n}^{(1)} + \cdots$ can readily be generated by making use of recursion formulae analogous to (5.14). A global frequency has therefore been obtained.

Note that type-1 and type-2 global frequencies correspond to the set Δ_1 in the complex ω plane introduced in § 3 (compare type-1 and type-2 Stokes line configurations sketched in figures $10a, b$ with those displayed on figures $4c, d$ and used to

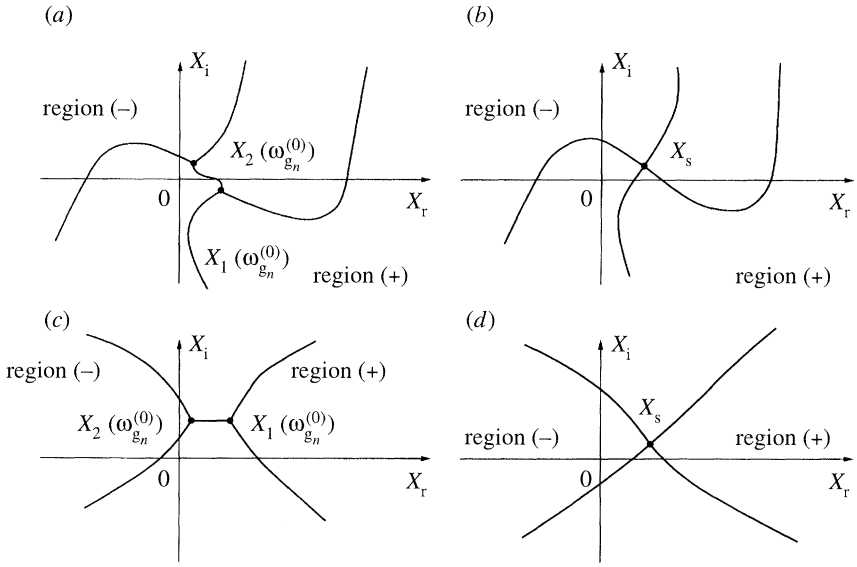

Figure 10. Stokes line networks in the complex X plane giving rise to global frequencies satisfying (5.16). They are transformed into the networks of the η plane, shown on figure 9, under the conformal mapping $X \mapsto \eta(X;\omega_{g_n}^{(0)})$: (*a*), $m > 0$, two simple turning points at $X_1(\omega_{g_n}^{(0)})$ and $X_2(\omega_{g_n}^{(0)})$; type-1 configuration; (*b*), $m = 0$, one double-turning point at the origin, type-2 configuration; (*c*), type-1 configuration with 'untwisted' Stokes lines; (*d*) type-2 configuration with 'untwisted' Stokes lines (see discussion following equation (5.37) in the text).

define the set Δ_1). For future reference, in § 5 *e*, we recall that the set Δ_1 is by definition included in the curve or set of curves Δ defined by condition (3.3) and it is the complement in Δ of the set Δ_0 of frequencies excluded by the necessary condition invoked in § 3. Condition (3.3) is then satisfied by all leading-order global frequencies $\omega_{g_n}^{(0)}$ and using expressions (2.6), (5.8) and (5.16), it also reads

$$\mathrm{Im}[\gamma_{0_0}(\omega_{g_n}^{(0)})] = 0. \tag{5.19}$$

Note that this relation could have been directly deduced from relation (5.16).

In closing this discussion, it should be emphasized that the present analysis is restricted to global frequencies satisfying $\omega_i > \omega_{i,\max}(\infty)$. If $\omega_i \leqslant \omega_{i,\max}(\infty)$, an essential step in the argumentation breaks down: we are unable to guarantee that regions $\eta(+;\omega)$ and $\eta(-;\omega)$ necessarily need to be non-contiguous at infinity in order to give rise to a global mode (§ 5 *b*).

A detailed evaluation of the global mode frequencies and eigenfunctions is undertaken in the following subsection for type-1 and type-2 configurations.

(*d*) *Global mode classification*

(i) *Global modes with two simple turning points (type-1)*

It is assumed that the Stokes line network is composed of two first-order turning points $X_1(\omega_{g_n}^{(0)})$ and $X_2(\omega_{g_n}^{(0)})$ connected by a common Stokes line and that regions (+) and (−) are not contiguous, as in figure 10*a*. According to the results of the previous subsection, the global frequencies $\omega_{g_n}(\varepsilon)$ admit expansions of the form (5.17) when $\varepsilon \ll 1$. The $O(1)$ term $\omega_{g_n}^{(0)}$ is given by (5.16) with m defined in (5.15) and $\eta_1(\omega)$ in

(5.8). It can be concluded that $\omega_{g_n}^{(0)}$ is a root of the equation

$$\frac{1}{2\pi}\oint_C \sqrt{2\frac{\omega_{g_n}^{(0)}-\omega_0(X)}{\omega_{kk}(X)}}\,\mathrm{d}X = m, \quad m>0, \tag{5.20}$$

where the branch cut of the square root joins both turning points $X_1(\omega_{g_n}^{(0)})$ and $X_2(\omega_{g_n}^{(0)})$ as specified in the comments preceding (5.8). Equivalently, the eigenvalue relation for the global frequencies $\omega_{g_n}(\varepsilon)$ is, at leading order in ε, given by

$$\frac{1}{2\pi\varepsilon}\oint_C \sqrt{2\frac{\omega_{g_n}^{(0)}-\omega_0(X)}{\omega_{kk}(X)}}\,\mathrm{d}X = n+\frac{1}{2}+O(1). \tag{5.21}$$

Equation (5.20) dictates that the branch of the square root in the integrand should be the one to yield a positive value of the integral. The function $\eta_1^2(\omega_{g_n}^{(0)})$ is therefore uniquely defined. Thus, among the four determinations of the mapping function $\eta(X;\omega)$ initially possible (see (5.9)), only two remain, say $\eta(X;\omega)$ and $-\eta(X;\omega)$. Although both give the same eigenvalue relation (5.20), only one of them is such that region $\eta(+;\omega)$ contains the positive real axis as specified in § 5 *c*.

From knowledge of $\omega_{g_n}^{(0)}$, one can deduce the first-order correction $\omega_{g_n}^{(1)}$ satisfying (5.18). The function $\gamma_{0_0}(\omega_{g_n}^{(0)})$ is equal to (5.20) and $\gamma_{0_1}(\omega_{g_n}^{(0)})$ is defined in (A 2) of Appendix A so that one obtains

$$\omega_{g_n}^{(1)} = \left(n+\frac{1}{2}-\frac{m}{\varepsilon} - \frac{\displaystyle\oint_C \left\{ \frac{R_1(X)}{\sqrt{R_0(X;\omega_{g_n}^{(0)})}} \right\} \mathrm{d}X}{\displaystyle\oint_C \left\{ 4\frac{\sqrt{R_0(X;\omega_{g_n}^{(0)})}}{\eta_1^2(\omega_{g_n}^{(0)})-\eta^2(X;\omega^{(0)})} \right\} \mathrm{d}X} \right) \times \left(\oint_C \frac{\mathrm{d}X}{\sqrt{R_0(X;\omega_{g_n}^{(0)})}\omega_{kk}(X)} \right)^{-1}. \tag{5.22}$$

Recall that $R_0(X;\omega)$ and $R_1(X)$ are defined in (4.3 *a*, *b*). The branch of the square root in the above integrands is the same as in (5.20).

It is worthwhile to notice the peculiar behaviour of the approximation scheme for type-1 global modes as ε tends to zero. According to (5.15), at a given real positive value of m, the expansion of $\omega_{g_n}(\varepsilon)$ refers to larger and larger values of the mode index n as $\varepsilon \to 0$. The function $n(\varepsilon)$ may for instance be defined as an integer distant by an amount n_0 from the integer part of m/ε, i.e.

$$n(\varepsilon) = \mathrm{IP}(m/\varepsilon)+n_0; \quad n_0 = 0, \pm 1, \pm 2, \ldots, \tag{5.23}$$

where $\mathrm{IP}(m/\varepsilon)$ denotes the integer part of m/ε. The integer n_0 may be seen as a local index. Each value of n_0 defines a global mode of leading order frequency $\omega_{g_n}^{(0)}$. If the variations of n are given by (5.23), condition (5.15) is satisfied, but the quantity $n(\varepsilon)-m/\varepsilon$ appearing in (5.18) and (5.22) fluctuates between n_0 and n_0+1 as $\varepsilon \to 0$. Thus, the first-order correction $\omega_{g_n}^{(1)}$ effectively oscillates between two limiting values with decreasing ε, while remaining of order unity.

As discussed in § 5 *e* (see figure 12*a*, in particular), it may very well happen that the curve Δ defined by (5.19) along which all global frequencies lie, exhibits a local

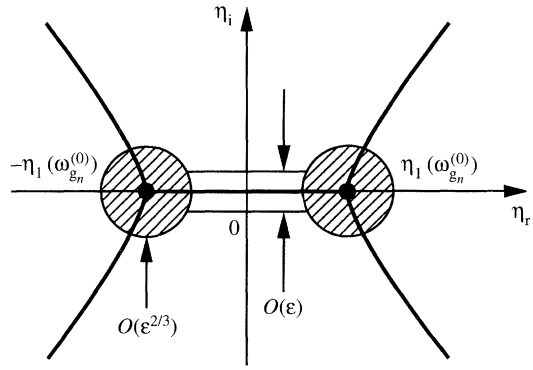

Figure 11. Domains in the complex η plane where the uniform approximation (5.24) of type-1 global eigenfunctions can be simplified: Hatched region, near a single turning point, approximation is given by expression (5.25) or (B 11); shaded region, near Stokes line, approximation is given by expression (5.26) or (B 12); elsewhere, approximation is given by expression (5.27) or (B 10).

maximum in the complex ω plane at a particular value $\omega_{g_n}^{(0)}$ satisfying (5.20). In this case, one necessarily has

$$\mathrm{Im}\left[\frac{\partial \gamma_{0_0}}{\partial \omega}(\omega_{g_n}^{(0)})\right] = 0$$

and, according to (5.18), the first-order correction $\omega_{g_n}^{(1)}$ has an imaginary part that is independent of n at a fixed value of ε, as long as $n \sim m/\varepsilon$. The expansion must be pursued to $O(\varepsilon^2)$ in order to catch growth rate variations $\mathrm{Im}\,\omega_{g_n}^{(2)}$ between the locally most unstable global modes. This behaviour is entirely consistent with simple scaling arguments: all global frequencies along the curve Δ_1 are separated by a distance $O(\varepsilon)$ around $\omega_{g_n}^{(0)}$, as given by (5.22), but, around a locally parabolic maximum, such a configuration only leads to $O(\varepsilon^2)$ variations in the growth rate.

We now proceed to the calculation of the eigenfunctions along the real X-axis. The spatial shape of type-1 global modes is given by the uniform approximation (5.1) with the expression (5.12) for $V(\xi)$. This spatial shape can be computed either for a given global frequency $\omega_{g_n}(\varepsilon)$ or for a given mode index $n(\varepsilon)$ since both are related through (5.13). Note however that the first two terms $\omega_{g_n}^{(0)}$ and $\omega_{g_n}^{(1)}$, given by relations (5.20) and (5.22), are sufficient to perfectly define the mode index $n(\varepsilon)$. Keeping only the leading-order terms in expansions (4.5 *a*, *b*) for $B(X;\omega,\varepsilon)$ and $C(X;\omega,\varepsilon)$, the uniform approximation (5.1) at a given frequency $\omega_{g_n}(\varepsilon)$ can be written as

$$\begin{aligned}\psi(X;\omega_{g_n},\varepsilon) = \Bigg\{ &\left(B_0(X;\omega_{g_n}) - \frac{1}{2}\eta(X;\omega_{g_n})C_0(X;\omega_{g_n})\right)\mathrm{He}_{n(\varepsilon)}\left[\frac{\eta(X;\omega_{g_n})}{\sqrt{\varepsilon}}\right] \\ &+\sqrt{\varepsilon}C_0(X;\omega_{g_n})\mathrm{He}'_{n(\varepsilon)}\left[\frac{\eta(X;\omega_{g_n}(\varepsilon))}{\sqrt{\varepsilon}}\right]\Bigg\} \\ &\times \exp\left(-\frac{\eta^2(X;\omega_{g_n})}{4\varepsilon}\right)\exp\left(\frac{\mathrm{i}}{\varepsilon}\int_{X_0}^{X} k_0(s)\,\mathrm{d}s\right), \end{aligned} \tag{5.24}$$

where $B_0(X;\omega)$ and $C_0(X;\omega)$ are given by (A 3 *a*,b). This approximation is valid in the entire complex X plane including both turning points $X_1(\omega_{g_n}^{(0)})$ and $X_2(\omega_{g_n}^{(0)})$.

It is also possible to deduce from (5.1) alternate expressions for the global mode eigenfunctions that remain uniformly valid only in specific subdomains of the complex

X plane. We recall that the index $n(\varepsilon)$ varies as m/ε when $\varepsilon \to 0$, where m is defined in (5.16) or (5.20). Thus, the behaviour of $\mathrm{He}_{n(\varepsilon)}(\eta/\sqrt{\varepsilon})$ appearing in $V_n(\eta/\sqrt{\varepsilon})$ and in (5.24) is highly singular since both the argument and the index become infinite as $\varepsilon \to 0$. As shown in Appendix B, it is possible to derive explicit asymptotic approximations for $V_{n(\varepsilon)}(\eta/\sqrt{\varepsilon})$ and $V'_{n(\varepsilon)}(\eta/\sqrt{\varepsilon})$ by applying the method of steepest descent to the integral representation of Hermite polynomials. The final results are summarized and discussed below.

Three distinct approximations are obtained depending on the location of X with respect to both turning points $X_1(\omega_{g_n}^{(0)})$ and $X_2(\omega_{g_n}^{(0)})$ and to the Stokes line that connects them. The different subdomains are represented in the complex η plane in figure 11.

Within discs of radius $O(\varepsilon^{2/3})$ around each turning point $\pm\eta_1(\omega_{g_n}^{(0)}) = \pm 2\sqrt{m}$ in the complex η plane (hatched areas in figure 11), the global mode eigenfunction is approximated by

$$\psi(X;\omega_{g_n},\varepsilon) \sim \alpha_0\sqrt{2\pi}(\pm 1)^n \left(\frac{m}{\varepsilon}\right)^{(n/2)+(1/6)} \mathrm{Ai}\left[\left(\frac{2\sqrt{2}m}{\varepsilon}\right)^{2/3}\left(\frac{\eta(X;\omega_{g_n})}{2\sqrt{m}} \mp 1\right)\right] \times \exp\left(-\frac{m}{\varepsilon}\left[\frac{3}{2} \mp \frac{\eta(X;\omega_{g_n})}{\sqrt{m}} + \frac{\eta^2(X;\omega_{g_n})}{4m}\right]\right) \times \exp\left(\frac{\mathrm{i}}{\varepsilon}\int_{X_0}^{X} k_0(s)\,\mathrm{d}s\right), \tag{5.25}$$

where $\mathrm{Ai}(x)$ denotes the usual Airy function. Correspondingly, in the complex X plane, the above result constitutes a valid approximation in circular neighbourhoods of radius $O(\varepsilon^{2/3})$ around each turning point $X_1(\omega_{g_n}^{(0)})$ and $X_2(\omega_{g_n}^{(0)})$. If, for instance, $X_1(\omega_{g_n}^{(0)})$ is mapped into $+\eta_1(\omega_{g_n}^{(0)})$, the upper sign in (5.25) pertains to the approximation near $X_1(\omega_{g_n}^{(0)})$ and the lower sign to the approximation near $X_2(\omega_{g_n}^{(0)})$.

Within a strip of width $O(\varepsilon)$ surrounding the Stokes line joining both turning points (shaded region in figure 11), the global mode approximation becomes

$$\psi(X,\omega_{g_n},\varepsilon) \sim \left\{\left[\frac{\eta+\sqrt{\eta^2-4m}}{2\sqrt{\varepsilon}}\right]^n \left[\frac{\eta+\sqrt{\eta^2-4m}}{\sqrt{\eta^2-4m}}\right]^{1/2} \times \exp(\mathrm{i}\Theta)\exp\left(-\frac{1}{4\varepsilon}\left(2m+\eta\sqrt{\eta^2-4m}\right)\right) + \left[\frac{\eta-\sqrt{\eta^2-4m}}{2\sqrt{\varepsilon}}\right]^n \left[\frac{\eta-\sqrt{\eta^2-4m}}{\sqrt{\eta^2-4m}}\right]^{1/2} \times \exp(-\mathrm{i}\Theta)\exp\left(-\frac{1}{4\varepsilon}\left(2m-\eta\sqrt{\eta^2-4m}\right)\right)\right\} \times \frac{\alpha_0}{\sqrt{2}}\left(\frac{\partial\eta}{\partial X}\right)^{-1/2} \exp\left(\frac{\mathrm{i}}{\varepsilon}\int_{X_0}^{X} k_0(s)\,\mathrm{d}s\right). \tag{5.26}$$

Elsewhere in the complex η or X plane the global mode admits a uniform expansion

given by

$$\psi(X,\omega_{g_n},\varepsilon)\sim\frac{\alpha_0}{\sqrt{2}}\left[\frac{\eta+\sqrt{\eta^2-4m}}{2\sqrt{\varepsilon}}\right]^n\left[\frac{\eta+\sqrt{\eta^2-4m}}{\sqrt{\eta^2-4m}}\right]^{1/2}\left(\frac{\partial\eta}{\partial X}\right)^{-1/2}\exp(\mathrm{i}\Theta)$$
$$\times\exp\left(-\frac{1}{4\varepsilon}\left(2m+\eta\sqrt{\eta^2-4m}\right)\right)\exp\left(\frac{\mathrm{i}}{\varepsilon}\int_{X_0}^{X}k_0(s)\,\mathrm{d}s\right).\quad(5.27)$$

The branch cut of the square root in the above formulae is fixed on the segment joining both turning points $\pm\eta_1(\omega_{g_n}^{(0)})=\pm2\sqrt{m}$ and the branch is chosen such that

$$-\tfrac{1}{2}\pi<\arg\left(\sqrt{\eta^2-4m}\right)\leqslant\tfrac{1}{2}\pi,\quad\text{when}\quad-\tfrac{1}{2}\pi<\arg(\eta)\leqslant\tfrac{1}{2}\pi.$$

We recall that α_0 and X_0 are arbitrary constants which can eventually be set by a normalization condition and that the positive number m defined as $\eta_1^2(\omega_{g_n}^{(0)})$ is also given by (5.20). The phase function $\Theta=\Theta(X;\omega_{g_n}^{(0)})$ in (5.26) and (5.27) is specified in (A 4).

Note that the uniformity of approximation (5.24) has been lost during this additional asymptotic expansion process and that the final results (5.25)–(5.27) are only local approximations. Near each turning point, the global mode approximation, given by (5.25), is an Airy-type solution. This result is not surprising in view of the fact that Airy functions generally appear in local one-turning-point analysis. Far away from the turning points, the global mode is given by (5.26) or (5.27). As discussed in Appendix B, these expressions are nothing but leading-order WKBJ approximations. One can indeed demonstrate that equation (5.26) is the sum of two WKBJ contributions built with the branches k^+ and k^- defined in (2.6). In the region where (5.26) is valid, i.e. near the Stokes line that connects the two turning points, both WKBJ approximations are of the same order of magnitude. It is then obvious that both must contribute to the eigenfunction. Far away from this Stokes line, approximation (5.27) consisting of a single WKBJ contribution must be used. It can readily be verified that the WKBJ approximation (5.27) is subdominant in regions (+) and (−) of the complex X plane and dominant in the other Stokes sectors. This feature is consistent with the necessary global mode existence condition obtained in § 3 and with the fact that WKBJ approximations defined as subdominant in the (+) and (−) subdomains remain valid in the adjacent Stokes sectors where they become dominant.

(ii) *Global modes with a double-turning point (type-2)*

If the Stokes line network involves a double-turning point X_s as in figure 10*b*, the results of Chomaz *et al.* (1991) and Monkewitz *et al.* (1993) are formally recovered. The procedure is briefly outlined below, particular attention being given to the correct choice of branches in the multiple-valued functions appearing at successive orders. Since X_s is a double-turning point, one has $X_1(\omega_s)=X_2(\omega_s)$ for a particular frequency ω_s. In other words, X_s is, by definition, a double root of equation (2.8), as discussed in § 2. It is therefore located at a saddle point of $\omega_0(X)$ such that

$$\omega_0(X_s)=\omega_s,\quad(5.28\,a)$$

$$\frac{\mathrm{d}\omega_0}{\mathrm{d}X}(X_s)=0.\quad(5.28\,b)$$

Note that the selection of type-2 global frequencies only relies on the local existence of a saddle point X_s of $\omega_0(X)$ in the complex X plane. By contrast, type-1 global

frequencies are selected on the basis of an integral (5.20) involving $\omega_0(X)$ and $\omega_{kk}(X)$ over an extended domain in the complex X plane.

The image of X_s is the double-turning point $\eta_1(\omega_s) = 0$ in the complex η plane, as illustrated in figure 9*b*. This property leads to a simple expression for the leading-order mapping function $\eta(X;\omega_{g_n}(\varepsilon))$: when $\eta_1 = 0$, equation (5.5) reduces to

$$\eta(X;\omega_{g_n}(\varepsilon)) = \eta(X;\omega_s) + \varepsilon r(X;\omega_{g_n}(\varepsilon)), \quad \text{with } r(X;\omega_{g_n}(\varepsilon)) = O(1), \tag{5.29}$$

where

$$\eta(X;\omega_s) = 2\left[\int_{X_s}^{X} \sqrt{2\frac{\omega_0(r)-\omega_s}{\omega_{kk}(r)}}\,\mathrm{d}r\right]^{1/2}. \tag{5.30}$$

In the present case, the square root function is analytic everywhere since, near X_s, $\omega_0(r) - \omega_s \sim \frac{1}{2}\omega^s_{0XX}(r - X_s)^2$. As before, the branch is chosen so that $\eta(+;\omega_s)$ contains the positive real η-axis, i.e. $-\frac{1}{4}\pi < \arg\eta < \frac{1}{4}\pi$ when X is in region (+).

Provided that $m = 0$, relation (5.16) for the leading-order global frequencies is identically satisfied since $\eta_1(\omega_s) = 0$. Higher order approximations to $\omega_{g_n}(\varepsilon)$ are generated by assuming an expansion of the form (5.17) with $\omega^{(0)}_{g_n} = \omega_s$. The first-order correction $\omega^{(1)}_{g_n}$ is given by (5.18). When $\eta(X;\omega_s)$ takes the form (5.30), expression (A 2) for $\gamma_{0_1}(\omega_s)$ can be calculated explicitly to yield

$$\gamma_{0_1}(\omega_s) = \frac{\mathrm{i}k^s_{0X}}{2}\sqrt{\frac{\omega^s_{kk}}{\omega^s_{0XX}}}, \tag{5.31}$$

where the superscript 's' indicates evaluation at the saddle point X_s.

The following simple reasoning ensures that the square root appearing in (5.31) is interpreted correctly. The determination chosen for $\sqrt{\omega^s_{kk}/\omega^s_{0XX}}$ should correspond to the branch selected for the mapping $\eta(X;\omega_s)$ in (5.30). A Taylor expansion of this relation in the immediate vicinity of X_s yields

$$\eta(X;\omega_s) \sim \left[4\frac{\omega^s_{0XX}}{\omega^s_{kk}}\right]^{1/4}(X - X_s). \tag{5.32}$$

According to the rule stated in connection with (5.30), the sector $\eta(+;\omega_s)$ in the vicinity of the origin, delimited by $-\frac{1}{4}\pi < \arg\eta < \frac{1}{4}\pi$, should map into the (+) sector close to X_s. As implied by (5.32), this sector is bounded by the straight lines

$$-\frac{\pi}{4} + \frac{1}{2}\arg\sqrt{\frac{\omega^s_{kk}}{\omega^s_{0XX}}} \leqslant \arg(X - X_s) \leqslant \frac{\pi}{4} + \frac{1}{2}\arg\sqrt{\frac{\omega^s_{kk}}{\omega^s_{0XX}}}. \tag{5.33}$$

The branch of the square root in (5.31) should therefore be such that $\frac{1}{2}\arg\sqrt{\omega^s_{kk}/\omega^s_{0XX}}$ *denotes a direction around* X_s *that points into region* (+) *or* (−) *of the complex* X *plane.*

The expression for $(\partial\gamma_{0_0}/\partial\omega)(\omega_s)$ reduces to

$$\frac{\partial\gamma_{0_0}}{\partial\omega}(\omega_s) = \frac{\varsigma}{\omega^s_{kk}}\sqrt{\frac{\omega^s_{kk}}{\omega^s_{0XX}}}, \tag{5.34}$$

where the square root is defined in the manner discussed above. The unknown $\varsigma = \pm 1$ has been added to account for the fact that (5.31) and (5.34) do not necessarily correspond to the same definition of the square root. Its value needs to be chosen

PHILOSOPHICAL TRANSACTIONS OF THE ROYAL SOCIETY A MATHEMATICAL, PHYSICAL & ENGINEERING SCIENCES

so that the branches in $(\partial\gamma_{0_0}/\partial\omega)(\omega_s)$ and $\gamma_{0_0}(\omega_s)$ are the same. Unfortunately, unlike type-1 configurations, the leading-order equation for the frequency reduces to $\gamma_{0_0}(\omega_s) = 0$: it is satisfied for both branches and a conclusion cannot be reached. We therefore leave ς temporarily undetermined and appeal to a different reasoning in order to settle this point, as discussed below.

Upon substituting the expressions (5.31) and (5.34) into (5.18), the first-order correction $\omega^{(1)}_{g_n}$ is found to be

$$\omega^{(1)}_{g_n} = \varsigma \left[-\frac{\mathrm{i}}{2} k^s_{0X} \omega^s_{kk} + (n + \tfrac{1}{2}) \omega^s_{kk} \sqrt{\frac{\omega^s_{0XX}}{\omega^s_{kk}}} \right], \tag{5.35}$$

where

$$\sqrt{\frac{\omega^s_{0XX}}{\omega^s_{kk}}}$$

is interpreted as

$$\left[\sqrt{\frac{\omega^s_{kk}}{\omega^s_{0XX}}} \right]^{-1},$$

which is defined in the sentence following (5.33). According to this result, $\omega_{g_n}(\varepsilon)$ moves away from ω_s as the mode index n increases, so that the type-2 Stokes line network (figure 10*b*) must gradually evolve into a type-1 configuration (figure 10*a*) with two distinct turning points $X_1[\omega_{g_n}(\varepsilon)]$ and $X_2[\omega_{g_n}(\varepsilon)]$. The expansion of the definition $\omega_0[X_j(\omega_{g_n}(\varepsilon))] = \omega_{g_n}(\varepsilon), j = 1, 2$, around X_s leads to the leading-order approximation

$$\tfrac{1}{2}\omega^s_{0XX}(X_j - X_s)^2 \sim \omega^{(1)}_{g_n}\varepsilon,$$

whereby the separation distance between X_1 and X_2 can be estimated as

$$[X_2(\omega_{g_n}) - X_1(\omega_{g_n})]^2 = 8\frac{\omega^{(1)}_{g_n}}{\omega^s_{0XX}}\varepsilon + O(\varepsilon^2). \tag{5.36}$$

As n increases, the two turning points move away from each other along a line of angle $\frac{1}{2}\arg[\omega^{(1)}_{g_n}/\omega^s_{0XX}]$, which, from (5.35), can be estimated as

$$\frac{1}{2}\arg\left\{\varsigma\sqrt{\frac{\omega^s_{kk}}{\omega^s_{0XX}}}\right\}$$

for sufficiently large n. In order to give rise to a type-1 configuration (figure 10*a*), this angle must lie within the sector (+) specified in (5.33) or the directly opposite sector (−). The value $\varsigma = 1$ must therefore be selected. It can be concluded that type-2 global frequencies form a discrete set given by

$$\omega_{g_n}(\varepsilon) \sim \omega_s + \varepsilon \left[-\frac{\mathrm{i}}{2} k^s_{0X} \omega^s_{kk} + (n + \tfrac{1}{2}) \omega^s_{kk} \sqrt{\frac{\omega^s_{0XX}}{\omega^s_{kk}}} \right] + O(\varepsilon^2), \tag{5.37}$$

where the square root is defined as in (5.35). It should be emphasized that in the configuration of figure 10*d*, this definition is equivalent to the selection of the square

root satisfying

$$\mathrm{Re}\sqrt{\frac{\omega^{\mathrm{s}}_{kk}}{\omega^{\mathrm{s}}_{0XX}}} > 0.$$

But in twisted configurations such as the one on figure 10*b*, this rule implies

$$\mathrm{Re}\sqrt{\frac{\omega^{\mathrm{s}}_{kk}}{\omega^{\mathrm{s}}_{0XX}}} < 0.$$

The variations of the growth rate with mode index n may now be determined in the vicinity of ω_{s}. If

$$\mathrm{Im}\left[\omega^{\mathrm{s}}_{kk}\sqrt{\frac{\omega^{\mathrm{s}}_{0XX}}{\omega^{\mathrm{s}}_{kk}}}\right] < 0,$$

the growth rate $\mathrm{Im}\,\omega_{\mathrm{g}_n}$ is maximum when $n = 0$, which corresponds to the most unstable type-2 global mode. If

$$\mathrm{Im}\left[\omega^{\mathrm{s}}_{kk}\sqrt{\frac{\omega^{\mathrm{s}}_{0XX}}{\omega^{\mathrm{s}}_{kk}}}\right] > 0,$$

the growth rate increases with the mode index n and type-2 global modes are not the most unstable, as discussed in § 5 *e*.

For any fixed n, the global mode eigenfunction of frequency ω_{g_n} admits the uniform approximation (5.1), which reduces at leading order in ε to

$$\psi(X;\omega_{\mathrm{g}_n},\varepsilon) \sim \left\{B_0(X;\omega_{\mathrm{g}_n})V_n\left[\frac{\eta(X;\omega_{\mathrm{g}_n})}{\sqrt{\varepsilon}}\right] + \sqrt{\varepsilon}C_0(X;\omega_{\mathrm{g}_n})V_n'\left[\frac{\eta(X;\omega_{\mathrm{g}_n})}{\sqrt{\varepsilon}}\right]\right\} \times \exp\left(\frac{\mathrm{i}}{\varepsilon}\int_{X_0}^{X} k_0(s)\,\mathrm{d}s\right), \tag{5.38}$$

where $B_0(X;\omega)$ and $C_0(X;\omega)$ are expressed in (A 3 *a*,*b*) and $V_n(\xi)$ is given by (5.12). Although this approximation is of the same form as for type-1 global modes, the computation for a given X is in the present case much easier because n is fixed. As outlined in Appendix C, expression (5.38) can be further simplified by making use of eigenrelation (5.37), definition (5.5) for the transformation $X \mapsto \eta(X;\omega)$, and expressions (A 3 *a*, *b*) for B_0 and C_0. According to (C 3) and (C 4), the final result can be expressed as

$$\psi(X;\omega_{\mathrm{g}_n},\varepsilon) \sim \alpha_0\left(\frac{\partial\eta}{\partial X}(X;\omega_{\mathrm{s}})\right)^{-1/2}\mathrm{He}_n\left[\frac{\eta(X;\omega_{\mathrm{s}})}{\sqrt{\varepsilon}}\right] \times \exp\left(\mathrm{i}\Theta(X;\omega_{\mathrm{s}}) - \frac{\omega^{(1)}_{\mathrm{g}_n}}{4\varepsilon}\frac{\partial(\eta^2)}{\partial\omega}(X;\omega_{\mathrm{s}})\right) \times \exp\left(-\frac{\eta^2(X;\omega_{\mathrm{s}})}{4\varepsilon}\right)\exp\left(\frac{\mathrm{i}}{\varepsilon}\int_{X_0}^{X} k_0(s)\,\mathrm{d}s\right). \tag{5.39}$$

We recall that $\eta(X;\omega_{\mathrm{s}})$, $\Theta(X;\omega_{\mathrm{s}})$ and $\omega^{(1)}_{\mathrm{g}_n}$ are given by (5.30), (A 4) and (5.35), respectively. The derivative $(\partial(\eta^2)/\partial\omega)(X;\omega_{\mathrm{s}})$ is computed in Appendix C and given by (C 6) and, as for type-1 global modes, α_0 and X_0 are constants that can be

arbitrarily specified. Expression (5.39), as expression (5.38), is valid in the entire complex X plane including the double-turning point X_{s}.

(*e*) *Frequency selection criteria*

In this subsection, necessary and sufficient conditions for global instability are examined in succession, together with frequency selection criteria.

(i) *Necessary condition for global instability*

From the previous analysis, one readily obtains an upper bound on the global mode growth rates

$$\omega_{\mathrm{g}_n,\mathrm{i}} \leqslant \omega_{0,\mathrm{i}}^{\max}, \tag{5.40}$$

where we recall that $\omega_{0,\mathrm{i}}^{\max}$ is the maximum value reached by the absolute growth rate on the real X-axis. The proof of this inequality directly follows from the nature of the Stokes line networks when $\omega_{\mathrm{i}} > \omega_{0,\mathrm{i}}^{\max}$, as sketched in figure 6*a*, *b*. These configurations fall within none of the types associated with global modes, as discussed in § 5 *c*, *d* and illustrated in figure 10, which proves inequality (5.40). This result already appeared as theorem 1 in Chomaz *et al.* (1991), but the proof was incomplete: configurations such as those of figure 6*b* were not explicitly shown not to correspond to global modes.

The following statement immediately follows from inequality (5.40): *if* $\omega_{0,\mathrm{i}}^{\max} < 0$, *the medium is globally stable*. In other words, *the presence of a region of absolute instability is a necessary condition for the existence of an amplified global mode*, as already argued in Chomaz *et al.* (1991).

(ii) *Sufficient conditions for global instability*

By summarizing the results of § 5 *d*, the following sufficient condition is obtained: if there exists a global mode of positive growth rate $\omega_{\mathrm{g,i}}$ that is associated with either two simple turning points (type-1) or a double-turning point (type-2), the medium is globally unstable.

If, in particular, the absolute frequency $\omega_0(X)$ admits a saddle point X_{s} defined by

$$\frac{\mathrm{d}\omega_0}{\mathrm{d}X}(X_{\mathrm{s}}) = 0,$$

and such that $\omega_{0,\mathrm{i}}(X_{\mathrm{s}}) > 0$, X_{s} is a double-turning point with a Stokes line network that is necessarily type-2. According to § 5 *d*, the complex absolute frequency $\omega_{\mathrm{s}} \equiv \omega_0(X_{\mathrm{s}})$ is then, at leading order in ε, a global frequency. The following sufficient condition therefore holds: *if the absolute frequency* $\omega_0(X)$ *presents a saddle point* X_{s} *with* $\omega_{0,\mathrm{i}}(X_{\mathrm{s}}) > 0$, *the medium is globally unstable.*

However, it should be emphasized that, in such circumstances, type-2 global modes are not necessarily the most amplified. *The most unstable global mode may correspond to a double-turning point type-2 configuration, in which case the dominant global frequency is given by formula (5.37) with* $n = 0$. *But, it may also very well correspond to a type-1 configuration with two simple turning points, in which case the global frequency is the root of equation (5.20) for a mode index* $n(\varepsilon) \sim m/\varepsilon$ *associated with a local maximum of* $\omega_{\mathrm{g}_n,\mathrm{i}}$.

In any case, *the leading-order approximation* $\omega_{\mathrm{g}}^{(0)}$ *to the most unstable global frequency is confined to the bounds*

$$\omega_{\mathrm{s,i}} \leqslant \omega_{\mathrm{g,i}}^{(0)} \leqslant \omega_{0,\mathrm{i}}^{\max}. \tag{5.41}$$

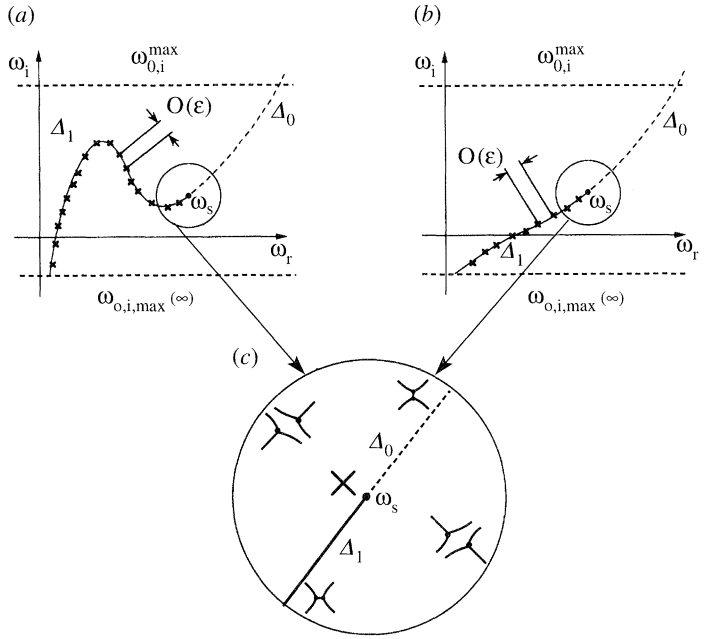

Figure 12. Sketches of possible global frequency distributions in complex ω plane. Curve Δ is defined by equation (3.3) in the text: – – –, Δ_0, 'no global mode' section of Δ; ——, Δ_1, 'global mode' section of Δ; ×, location of type-1 global mode; •, type-2 global mode. (*a*) most unstable global mode is type-1; (*b*) most unstable global mode is type-2; (*c*) Qualitative changes in Stokes line network of the complex η plane as ω is displaced around ω_s.

This result only holds when $\omega_{g,i}^{(0)} > \omega_i^{max}(\infty)$, as pointed out in § 5 *c*.

(iii) *Geometrical interpretation*

It has been shown that Stokes line configurations giving rise to global modes present either a double-turning point (figures 10*b*, *d*) or two simple turning points connected by a common Stokes line (figures 10*a*, *c*). This property has enabled us to prove that all global modes frequencies lie on the curve Δ in the complex ω plane defined by the single condition (5.19) that both turning points are connected by a Stokes line. Furthermore, as mentioned in § 5 *c*, if we partition the curve Δ into 'no global mode' and 'global mode' sections (dashed lines and solid lines on figure 12, respectively), the 'no global mode' and 'global mode' sections correspond, respectively, to the sets Δ_0 and Δ_1 introduced in § 3.

All frequencies on the 'no global mode' section are then such that regions (+) and (−) are contiguous, as illustrated on figure 12*c*. By contrast, all frequencies on the 'global mode' section are such that regions (+) and (−) are not contiguous. In such situations, we have demonstrated the existence of a denumerable set of type-1 global frequencies that are spaced within $O(\varepsilon)$ of each other. It can further be shown that 'global mode' and 'no global mode' sections are separated by a type-2 global frequency ω_s. Qualitative changes in the Stokes line network can easily be traced in the complex η plane (figure 12*c*). When ω travels along the curve Δ from the 'global mode' to the 'no global mode' sides, the two turning points $\eta_1(\omega)$ and $-\eta_1(\omega)$ collide at the origin and re-emerge on the vertical η-axis in a 'no global mode' configuration. Finally, for frequencies lying outside the curve Δ, the Stokes line connection between both turning points is broken, as sketched in figure 12*c*.

Two distinct situations (figure 12*a*, *b*) may now be envisioned for the shape of the curve Δ. If the 'global mode' section of Δ exhibits a local maximum sufficiently far away from ω_s, at a complex frequency $\omega^{(0)}$ such that $\omega_i^{(0)} > \omega_{s,i}$ (figure 12*a*), the most unstable global mode is necessarily type-1. If that local maximum is lower that $\omega_{s,i}$ or is absent, the most unstable global frequency is then type-2 (figure 12*b*).

Note that, near a type-1 local maximum, unstable global modes exhibit growth rates differing by $O(\varepsilon^2)$, in agreement with the analysis of § 5 *d*. If the most unstable global mode is type-2, the growth rates of neighbouring modes are separated by $O(\varepsilon)$, as can be observed from (5.37).

6. Discussion and conclusions

The main results of this investigation may be summarized in the following way. Global frequency selection criteria have been established for a class of systems governed by the linearized Ginzburg–Landau equation with slowly varying coefficients, when at most two turning points influence the spatial structure of perturbations in physical space. The complex frequencies of unstable global modes fall within two broad classes, according to the nature of the Stokes line network in the complex X plane. Type-1 global modes are associated with two simple turning points connected by a common Stokes line with no contiguous (+) and (−) regions. Corresponding frequencies are the roots of eigenvalue relation (5.21) with $n = O(1/\varepsilon)$. Type-2 global modes arise when both turning points merge into a double-turning point X_s. Selected frequencies are then given by (5.37), where $\omega_s = \omega_0(X_s)$ is defined by the saddle point condition (5.28 *b*). The most unstable global mode may either be type-1 (figure 12*a*) or type-2 (figure 12*b*), depending on the shape of the curve(s) supporting the eigenvalues in the complex ω plane. Finally, by reducing the Ginzburg–Landau equation to a single comparison equation, uniformly valid approximations to the spatial eigenfunctions have been derived, in a domain containing both turning points.

The analysis of Chomaz *et al.* (1991) has been extended significantly in several respects. First, Chomaz *et al.* (1991) limited their study to type-2 global modes. More specifically, the Stokes line network was explicitly assumed to be of the 'untwisted' kind (assumption 2 and figure 5 of Chomaz *et al.* 1991), which allowed one to prove that the most unstable global frequency is necessarily type-2 and given by ω_s. This restriction has been lifted here (compare figure 10*b* and figure 5 of Chomaz *et al.* 1991), and, as a result, it can be concluded that, in all generality, *the most unstable global mode may be type-1 or type-2*. Note that type-2 global frequencies (5.37) are identical to those calculated in Chomaz *et al.* (1991). Second, the leading-order approximation to the largest global growth rate is bounded from above by the maximum absolute growth rate $\omega_{0,i}^{\max}$ and from below by the growth rate $\omega_{s,i}$ at the saddle point X_s. The proof for the validity of the upper bound presented in Chomaz *et al.* (1991) has been completed. Third, instead of matching separate outer WKBJ expansions to inner expansions close to the turning points, we have obtained a single uniformly valid approximation for both type-1 and type-2 global mode eigenfunctions.

The present work has been restricted to the Ginzburg–Landau model equation with varying coefficients in a single space dimension. In order to be directly applicable to real flow situations, the cross-stream structure of the perturbations should be included within the setting of a linearized two-dimensional instability analysis around a slowly diverging basis flow. Such a formulation has recently been presented by Monkewitz *et al.* (1993) for type-2 global modes in a streamwise domain that is

PHILOSOPHICAL TRANSACTIONS OF THE ROYAL SOCIETY A MATHEMATICAL, PHYSICAL & ENGINEERING SCIENCES

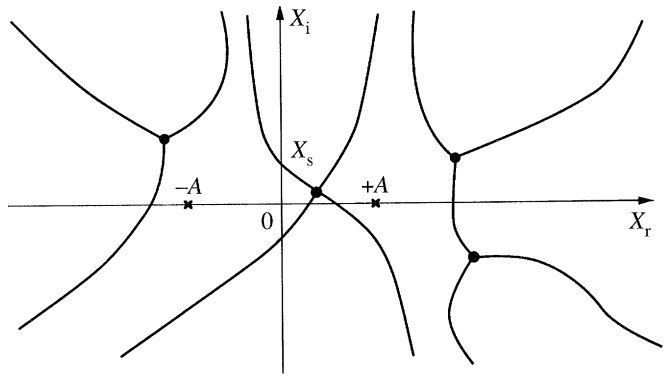

Figure 13. Example of domain reduction to a two-turning-point problem. The regions (+) and (−) are transferred in the neighbourhood of the saddle point X_s of $\omega_0(X)$ to the regions delimited by Stokes lines containing the points $-A$ and $+A$, respectively.

doubly infinite. It is then found that type-2 global frequencies remain formally given by (5.37), the cross-stream structure being 'slaved' to the streamwise evolution of the fluctuations. Note, however, that, in contrast with (5.37), the global frequency expansion (6.1) of Monkewitz *et al.* (1993) contains one additional frequency shift $\varepsilon\delta\omega^t$ associated with non-parallel flow effects. A similar term could have been obtained in the context of the Ginzburg–Landau model by postulating the existence of $O(\varepsilon)$ correction terms in the statement (2.1) of the problem. No comparable two-dimensional study of type-1 global modes has yet been undertaken and it remains to be determined whether type-1 eigenrelation (5.21) stays unchanged.

Experimental and numerical validations of the above global frequency selection criteria have been scarce and, for the most part, limited to testing the type-2 saddle point criterion of Chomaz *et al.* (1991). There is so far no evidence that type-1 global modes might dominate the dynamics of a specific spatially developing shear flow, but such structures have not actively been looked for. We therefore restrict the discussion to the validation of the type-2 criterion with the underlying provisional assumption that type-1 global modes are less unstable (figure 12*b*). It should also be emphasized that the present results as well as those of Monkewitz *et al.* (1993) rely heavily on a weak inhomogeneity assumption that may not always be strictly satisfied. Some caution must therefore be exercised when applying the frequency selection criterion to shear flows such as wakes at low Reynolds numbers.

The numerical simulations of Hannemann & Oertel (1989) clearly demonstrate that, in the case of the wake behind a plate of thickness h, the computed global frequency is nearly equal to the absolute frequency taken at the location $x/h = 1$. As discussed in Monkewitz *et al.* (1993), the absolute frequency $\omega_0(X)$ exhibits a saddle point close to that location and the present type-2 saddle point criterion is then in good agreement with numerical observations. Note also that the computed global frequency is very close to the absolute frequency at the transition point between absolute and convective instability (Koch's (1985) criterion). More recently, Schär & Smith (1993) have numerically investigated the flow behind a vertical circular cylinder in the shallow-water wave regime. At a critical value of the Froude number, the wake is observed to undergo a transition to large-scale Kármán vortex shedding. When all nonlinear terms in the numerical code are turned off, the wake beats at a global frequency $\omega_g \approx 0.17 + 0.045\mathrm{i}$. Local stability calculations performed on the unstable basic state then indicate the presence of a broad region of absolute

PHILOSOPHICAL TRANSACTIONS OF THE ROYAL SOCIETY A MATHEMATICAL, PHYSICAL & ENGINEERING SCIENCES

instability behind the obstacle. The function $\omega_0(X)$ can be estimated from a parabolic fit near the maximum absolute growth rate and application of criterion (5.28 *a*, *b*) leads to the prediction $\omega_g \approx 0.19 + 0.040\mathrm{i}$, which compares very favourably with the computed value. Note, however, that, when all nonlinearities are restored, the observed Strouhal frequency becomes $\omega_g \approx 0.27$, which is noticeably different from the predicted value. A similar approach has been applied by Huerre & Monkewitz (1990) to estimate the frequency of the preferred mode in two-dimensional jets from experimental data. As in the preceding case, the reconstruction of $\omega_0(X)$ from a parabolic fit leads to $\omega_g \approx 0.225$ to be compared with the measured value $\omega_g \approx 0.25$.

The above validation procedure can only be viewed as preliminary. A more thorough implementation of the frequency selection criteria requires a careful analytic continuation of the local quantities $\omega_0(X)$, $k_0(X)$, etc. from the real X-axis into the complex X plane. Unfortunately, the number, location and structure of turning points are very sensitive to slight changes in the numerical or experimental data on the real X-axis. This sensitivity becomes particularly acute when turning points that are implicated in the global mode structure, i.e. those with at least one Stokes line crossing the real X-axis, are located far into the complex X plane. It is then practically impossible to determine how many turning points are involved and their respective locations. In the favourable case where a saddle point X_s lies close to the real axis, one might envision reducing the physical domain of interest on the real axis to a finite segment around X_s, say $|X| < A$, as shown on figure 13.

The (+) and (−) regions could then be defined as those containing $X = A$ and $X = -A$, respectively, and a subdominant solution could be built on the finite interval as long as no other turning point is involved.

In the experiments on wakes, low-density jets and counterflow mixing layers alluded to in the introduction, global modes are isolated and seem to set in via a Hopf bifurcation, the modal amplitude being governed by a Landau equation close to onset, to a very good degree of approximation. Preliminary studies of weakly nonlinear effects for type-2 global modes have been undertaken by Chomaz *et al.* (1990) and Le Dizès *et al.* (1993) in the context of the present Ginzburg–Landau model. The results indicate that the Landau equation has a severely restricted range of validity in the limit of weak spatial non-uniformities, unless restrictive assumptions are made concerning the location of the saddle point X_s. In such a case, one may further include the cross-stream structure and extend the weakly nonlinear analysis to two-dimensional spatially developing flows in the viscous critical layer regime (Le Dizès *et al.* 1991).

The authors thank P. G. Drazin for drawing their attention to early pertinent work on global modes. They are grateful to M. Pesenson for many helpful discussions. They are also indebted to Colonel Buck Danny and Major Sonny Tucson for their useful comments on the final manuscript.

This investigation was supported by the Direction des Recherches, Etudes et Techniques of the French Ministry of Defense under Grants # 90-040 and 92-098 (S.L.D., P.H., J.M.C.), by SNECMA (S.L.D.), by the US Office of Naval Research under Grant # N00014-90-J-1313 (S.L.D., P.A.M.) and by AFOSR under Grant # F49620-92-J-0471 (P.A.M.). The Laboratoire d'Hydrodynamique (LadHyX) is part of URA 317 of the CNRS.

Appendix A. Some analytical results for the two-turning-point problem

In the following, a few analytical results pertaining to the two-turning-point problem are extracted from the earlier study by Lynn & Keller (1970). The functions

$R_0(X;\omega)$ and $R_1(X)$ that repeatedly appear in the expressions below, have been defined in (4.3 a, b) in terms of the local dispersion relation characteristics.

The first-order term $\gamma_{0_1}(\omega)$ in expansion (5.3) is given by (LK 6.21) as follows:

$$\gamma_{0_1}(\omega) = \frac{\displaystyle\int_{X_1(\omega)}^{X_2(\omega)} R_1(X)/\sqrt{R_0(X;\omega)}\,\mathrm{d}X}{\displaystyle\int_{X_1(\omega)}^{X_2(\omega)} 4\sqrt{R_0(X;\omega)}/[\eta_1^2(\omega)-\eta^2(X;\omega)]\,\mathrm{d}X}, \tag{A 1}$$

where the integration path joining $X_1(\omega)$ to $X_2(\omega)$ should avoid crossing the branch cut of the square root and be identical for both integrals. With the use of a closed contour C encircling both turning points, this expression can be rewritten as

$$\gamma_{0_1}(\omega) = \frac{\displaystyle\oint_C R_1(X)/\sqrt{R_0(X;\omega)}\,\mathrm{d}X}{\displaystyle\oint_C 4\sqrt{R_0(X;\omega)}/[\eta_1^2(\omega)-\eta^2(X;\omega)]\,\mathrm{d}X}. \tag{A 2}$$

The leading-order terms $B_0(X;\omega)$ and $C_0(X;\omega)$ in expansions (4.5 a, b) for $B(X;\omega,\varepsilon)$ and $C(X;\omega,\varepsilon)$ are given by expressions (LK 3.10) and (LK 3.11) as

$$B_0(X;\omega) = \alpha_0 \left[\frac{\partial \eta}{\partial X}(X;\omega)\right]^{-1/2} \cos\Theta(X;\omega), \tag{A 3 a}$$

$$C_0(X;\omega) = \alpha_0 \left[\frac{\partial \eta}{\partial X}(X;\omega)\right]^{1/2} [R_0(X;\omega)]^{-1/2} \sin\Theta(X;\omega), \tag{A 3 b}$$

with $\Theta(X;\omega)$ defined by (LK 6.20) as

$$\Theta(X;\omega) = \frac{1}{2}\int_{X_1(\omega)}^{X} \left[\frac{R_1(X)}{R_0^{1/2}(X;\omega)} - \frac{4\gamma_{0_1}(\omega)R_0^{1/2}(X;\omega)}{\eta_1^2(\omega)-\eta^2(X;\omega)}\right] \mathrm{d}X. \tag{A 4}$$

Note that function $\Theta(X;\omega)$ satisfies $\Theta(X_1(\omega),\omega) = \Theta(X_2(\omega),\omega) = 0$ by the definition of $\gamma_{0_1}(\omega)$.

Appendix B. Type-1 global eigenfunctions

In this appendix, the uniform approximation (5.24) for type-1 global modes is reduced by deriving, when $\varepsilon \to 0$, appropriate asymptotic expansions of $\mathrm{He}_{n(\varepsilon)}(\eta/\sqrt{\varepsilon})$ and $\mathrm{He}'_{n(\varepsilon)}(\eta/\sqrt{\varepsilon})$. The underlying idea is to seek further approximations for the functions $V_{n(\varepsilon)}(\eta/\sqrt{\varepsilon})$ and $V'_{n(\varepsilon)}(\eta/\sqrt{\varepsilon})$ defined in (5.12), in the limit $\varepsilon \to 0$, bearing in mind that $n(\varepsilon) \sim m/\varepsilon$. For this purpose, it is convenient to evaluate the Hermite polynomials $\mathrm{He}_{n(\varepsilon)}(\eta/\sqrt{\varepsilon})$ by applying the method of the steepest descent to their integral representation. The results are then substituted into (5.1) to generate local approximations for the global mode eigenfunctions in different regions of the complex X plane.

The integral representation of $\mathrm{He}_n(x)$ given in Bender & Orszag (1978, p. 574) reads

$$\mathrm{He}_n(x) = \sqrt{\frac{2}{\pi}}\mathrm{e}^{x^2/2}\int_0^{+\infty} \mathrm{e}^{-r^2/2} r^n \cos(rx - n\pi/2)\,\mathrm{d}r,$$

equivalently

$$\mathrm{He}_n(x) = \frac{1}{2}\sqrt{\frac{2}{\pi}}\mathrm{e}^{x^2/2}\int_{-\infty}^{+\infty}\mathrm{e}^{-r^2/2}r^n\mathrm{e}^{\mathrm{i}rx-\mathrm{i}n\pi/2}\,\mathrm{d}r. \tag{B 1}$$

Upon substituting (B 1) into (5.12), one obtains

$$V_{n(\varepsilon)}(\eta/\sqrt{\varepsilon}) = \frac{1}{2}\sqrt{\frac{2}{\pi}}\mathrm{e}^{-\mathrm{i}n\pi/2}\left[\frac{2m}{\varepsilon}\right]^{n+1/2}\mathrm{e}^{-\eta^2/(4\varepsilon)}\int_{-\infty}^{+\infty}r^{n-(m/\varepsilon)} \times \exp\left(-\frac{m}{\varepsilon}\left[(r-\frac{\mathrm{i}\eta}{\sqrt{2m}})^2-\ln r\right]\right)\mathrm{d}r,$$

$$V'_{n(\varepsilon)}(\eta/\sqrt{\varepsilon}) = \frac{1}{2}\sqrt{\frac{2}{\pi}}\mathrm{e}^{-\mathrm{i}n\pi/2}\left[\frac{2m}{\varepsilon}\right]^{n+1/2}\mathrm{e}^{-\eta^2/(4\varepsilon)}\int_{-\infty}^{+\infty}\left(\frac{\eta}{2\sqrt{\varepsilon}}+\mathrm{i}\sqrt{\frac{2m}{\varepsilon}}r\right)r^{n-(m/\varepsilon)} \times \exp\left(-\frac{m}{\varepsilon}\left[(r-\frac{\mathrm{i}\eta}{\sqrt{2m}})^2-\ln r\right]\right)\mathrm{d}r.$$

These expressions can be recast into the following compact form:

$$V_{n(\varepsilon)}(\eta/\sqrt{\varepsilon}) = C_\varepsilon^{(n)}I_\varepsilon^{(n)}(\eta)\mathrm{e}^{-\eta^2/(4\varepsilon)}, \tag{B 2 a}$$

$$V'_{n(\varepsilon)}(\eta/\sqrt{\varepsilon}) = C_\varepsilon^{(n)}\left[\mathrm{e}^{\mathrm{i}\pi/2}\sqrt{\frac{2m}{\varepsilon}}I_\varepsilon^{(n+1)}(\eta)+\frac{\eta}{2\sqrt{\varepsilon}}I_\varepsilon^{(n)}(\eta)\right]\mathrm{e}^{-\eta^2/(4\varepsilon)}, \tag{B 2 b}$$

with

$$I_\varepsilon^{(n)}(\eta) = \int_{-\infty}^{+\infty}r^{n-m/\varepsilon}\exp\left(-\frac{m}{\varepsilon}f(r;\eta)\right)\mathrm{d}r, \tag{B 3 a}$$

$$C_\varepsilon^{(n)} = \frac{1}{2}\sqrt{\frac{2}{\pi}}\mathrm{e}^{-\mathrm{i}n\pi/2}\left[\frac{2m}{\varepsilon}\right]^{(n+1)/2}, \tag{B 3 b}$$

$$f(r;\eta) = \left(r-\frac{\mathrm{i}\eta}{\sqrt{2m}}\right)^2-\ln r. \tag{B 3 c}$$

The behaviour of the integral $I_\varepsilon^{(n)}(\eta)$ when $\varepsilon\to 0$ can be determined by applying the method of steepest descent to the function $f(r;\eta)$, the variations of the factors appearing in front of the exponentials being negligible when $n-m/\varepsilon \ll m/\varepsilon$. As explained in standard text books (Bender & Orszag 1978, ch. 6), the principle of the method consists in deforming the contour of integration into lines $\mathrm{Im}[f(r;\eta)] =$ const. which are also steepest-descent paths of $\mathrm{Re}[f(r;\eta)]$, and searching for the saddle point(s) $r(\eta)$ where $\mathrm{Re}[f(r;\eta)]$ reaches a minimum on that path. The main contribution to the integral as $\varepsilon\to 0$ is then found to arise from the neighbourhood of the saddle points $r(\eta)$ satisfying the condition

$$\frac{\partial f}{\partial r}(r(\eta);\eta) = 0.$$

In the present case, expression (B 3 *c*) tells us that the function $f(r;\eta)$ admits only two saddle points, given by

$$r^{\pm}(\eta) = \frac{\mathrm{i}\eta\pm\mathrm{i}\sqrt{\eta^2-4m}}{2\sqrt{2m}}. \tag{B 4}$$

When $r^+(\eta)$ and $r^-(\eta)$ are distinct, there exist two possible candidates for the leading-order approximation to $I_\varepsilon^{(n)}(\eta)$ as $\varepsilon \to 0$:

$$I_\varepsilon^{(n)\pm}(\eta) = [r^\pm(\eta)]^{n-m/\varepsilon} \exp\left(-\frac{m}{\varepsilon} f(r^\pm(\eta);\eta)\right) \sqrt{\frac{2\pi\varepsilon}{m\partial_{\rm r}^2 f(r^\pm(\eta);\eta)}}. \tag{B 5}$$

These expressions have been obtained by expanding the function $f(r;\eta)$ near each saddle point $r^\pm(\eta)$ according to

$$f(r;\eta) = f(r^\pm(\eta);\eta) + \tfrac{1}{2}(r - r^\pm(\eta))^2 \partial_{\rm r}^2 f(r^\pm(\eta);\eta) + \cdots,$$

the contribution to the integral $I_\varepsilon^{(n)}(\eta)$ from each saddle point being then a trivial Gaussian integral.

If one proceeds to a detailed analysis of the topography of the $\mathrm{Im}[f(r;\eta)] = \text{const.}$ contours, one can in fact show that the leading-order contribution to the integral $I_\varepsilon^{(n)}(\eta)$ always arises from the neighbourhood of the same saddle point $r^+(\eta)$, if the branch cut and branch of the square root in (B 4) are chosen to be the interval $[-2\sqrt{m}, 2\sqrt{m}]$ of the real $\eta_{\rm r}$-axis and such that

$$-\tfrac{1}{2}\pi < \arg(\sqrt{\eta^2 - 4m}) \leqslant \tfrac{1}{2}\pi, \quad \text{when } -\tfrac{1}{2}\pi < \arg(\eta) \leqslant \tfrac{1}{2}\pi. \tag{B 6}$$

Thus, for that particular determination, we obtain

$$I_\varepsilon^{(n)}(\eta) \sim I_\varepsilon^{(n)+}(\eta). \tag{B 7}$$

Nevertheless, there are two localized regions in the complex η plane where this approximation is not valid (see figure 11).

The first region is for η values close to the turning points $\pm 2\sqrt{m} = \pm\eta_1(\omega_{{\rm g}n}^{(0)})$. At turning points, both saddle points $r^+(\eta)$ and $r^-(\eta)$ collide at a single point $r_0(\pm 2\sqrt{m}) = \pm \mathrm{i}/\sqrt{2}$ to create a zero of $f(r;\eta)$ of order two such that $\partial_{\rm r} f(r_0(\pm 2\sqrt{m}); \pm 2\sqrt{m}) = 0$ and $\partial_{\rm r}^2 f(r_0(\pm 2\sqrt{m}); \pm 2\sqrt{m}) = 0$. Note in particular that the function $1/\partial_{\rm r}^2 f(r^+(\eta),\eta)$, being infinite at $\eta = \pm 2\sqrt{m}$, the approximation (B 5) for $I_\varepsilon^{(n)}(\eta)$ could not possibly remain valid. In discs of radius $O(\varepsilon^{2/3})$ around each turning point $\pm 2\sqrt{m}$, $I_\varepsilon^{(n)}(\eta)$ is found to be of the form

$$I_\varepsilon^{(n)}(\eta) \sim 2\pi \left(\frac{\varepsilon}{2\sqrt{2}m}\right)^{1/3} \left(\frac{\pm\mathrm{i}}{\sqrt{2}}\right)^n \exp\left(\frac{m(-3 \pm 2\eta/\sqrt{m})}{2\varepsilon}\right) \times \mathrm{Ai}\left[\left(\frac{2\sqrt{2}m}{\varepsilon}\right)^{2/3} \left(\frac{\eta}{2\sqrt{m}} \mp 1\right)\right], \tag{B 8}$$

where the upper and lower signs refer to approximations near $+2\sqrt{m}$ and $-2\sqrt{m}$, respectively. To derive approximation (B 8), $f(r;\eta)$ is expanded around the second-order saddle point $r_0(\pm 2\sqrt{m}) = \pm\mathrm{i}/\sqrt{2}$ that gives the dominant contribution to the integral as done in order to obtain (B 5). The expression (B 8) is then easily generated from (B 3 *a*) if one further recalls the following integral representation for Ai (Bender & Orszag 1978, p. 313):

$$\mathrm{Ai}(x) = \frac{1}{2\pi\mathrm{i}} \int_{\infty \mathrm{e}^{-2\pi\mathrm{i}/3}}^{\infty \mathrm{e}^{2\pi\mathrm{i}/3}} \mathrm{e}^{xs - s^3/3}\, \mathrm{d}s.$$

The approximation (B 7) is also not valid in a strip of width $O(\varepsilon)$ along the Stokes

line connecting both turning points $\pm 2\sqrt{m} = \pm\eta_1(\omega_{g_n}^{(0)})$. For values of η in that region, the contour of integration deformed along the lines $\mathrm{Im}[f(r;\eta)] = \text{const.}$ goes through both saddle points $r^+(\eta)$ and $r^-(\eta)$ and the contributions from each to the integral (B 3 *a*) are found to be of the same order. Approximation to $I_\varepsilon^{(n)}(\eta)$ then does not reduce to a single contribution from the saddle point $r^+(\eta)$ but to the sum of both contributions from $r^+(\eta)$ and $r^-(\eta)$:

$$I_\varepsilon^{(n)}(\eta) \sim I_\varepsilon^{(n)+}(\eta) + I_\varepsilon^{(n)-}(\eta). \tag{B 9}$$

Everywhere in the complex η plane, except close to both turning points $\pm 2\sqrt{m}$ and close to the Stokes line that connects them (hatched and shaded regions in figure 11, respectively), $I_\varepsilon^{(n)}(\eta)$ is given by (B 7). The functions $V_{n(\varepsilon)}(\eta/\sqrt{\varepsilon})$ and $V'_{n(\varepsilon)}(\eta/\sqrt{\varepsilon})$ can then be computed using (B 2 *a*, *b*) and the uniform approximation (5.24) for the global mode reduces to

$$\psi \sim C_\varepsilon^{(n)} I_\varepsilon^{(n)+}(\eta)[B_0 + (\mathrm{e}^{\mathrm{i}\pi/2}\sqrt{2m}r^+(\eta) + \tfrac{1}{2}\eta)C_0] \exp\left(-\frac{\eta^2}{4\varepsilon}\right) \exp\left(\frac{\mathrm{i}}{\varepsilon}\int_{X_0}^{X} k_0(s)\,\mathrm{d}s\right).$$

From expressions (A 3 *a*, *b*) for B_0 and C_0 and the relation

$$\mathrm{i}\frac{\partial\eta}{\partial X}\sqrt{\eta^2 - 4m} = 2\sqrt{R_0}$$

obtained by differentiating (5.5) with respect to X, the expression within brackets can be simplified as

$$[B_0 + (\mathrm{e}^{\mathrm{i}\pi/2}\sqrt{2m}r^+(\eta) + \tfrac{1}{2}\eta)C_0] = \alpha_0 \left(\frac{\partial\eta}{\partial X}\right)^{-1/2} \mathrm{e}^{\mathrm{i}\Theta}.$$

It immediately follows that

$$\begin{aligned}\psi(X;\omega_{g_n},\varepsilon) \sim \frac{\alpha_0}{\sqrt{2}} &\left[\frac{\eta + \sqrt{\eta^2 - 4m}}{2\sqrt{\varepsilon}}\right]^n \left[\frac{\eta + \sqrt{\eta^2 - 4m}}{\sqrt{\eta^2 - 4m}}\right]^{1/2} \\ &\times \left(\frac{\partial\eta}{\partial X}\right)^{-1/2} \mathrm{e}^{\mathrm{i}\Theta} \exp\left(-\frac{1}{4\varepsilon}(2m + \eta\sqrt{\eta^2 - 4m})\right) \\ &\times \exp\left(\frac{\mathrm{i}}{\varepsilon}\int_{X_0}^{X} k_0(s)\,\mathrm{d}s\right).\end{aligned} \tag{B 10}$$

In the vicinity of the turning points $\pm 2\sqrt{m}$, using the expression (B 8) for $I_\varepsilon^{(n)}(\eta)$, the uniform approximation reduces to

$$\begin{aligned}\psi(X;\omega_{g_n},\varepsilon) \sim \alpha_0\sqrt{2\pi}(\pm 1)^n &\left(\frac{m}{\varepsilon}\right)^{(n/2)+(1/6)} \\ &\times \mathrm{Ai}\left[\left(\frac{2\sqrt{2}m}{\varepsilon}\right)^{2/3}\left(\frac{\eta}{2\sqrt{m}} \mp 1\right)\right] \\ &\times \exp\left(-\frac{m}{\varepsilon}\left[\frac{3}{2} \mp \frac{\eta}{\sqrt{m}} + \frac{\eta^2}{4m}\right]\right) \exp\left(\frac{\mathrm{i}}{\varepsilon}\int_{X_0}^{X} k_0(s)\,\mathrm{d}s\right).\end{aligned} \tag{B 11}$$

Finally, near the Stokes line connecting $\pm 2\sqrt{m}$, by making use of (B 9), the uniform

approximation is obtained as

$$\psi(X,\omega_{g_n},\varepsilon)\sim\left\{\left[\frac{\eta+\sqrt{\eta^2-4m}}{2\sqrt{\varepsilon}}\right]^n\left[\frac{\eta+\sqrt{\eta^2-4m}}{\sqrt{\eta^2-4m}}\right]^{1/2}\right.$$
$$\times e^{i\Theta}\exp\left(-\frac{1}{4\varepsilon}(2m+\eta\sqrt{\eta^2-4m})\right)$$
$$+\left[\frac{\eta-\sqrt{\eta^2-4m}}{2\sqrt{\varepsilon}}\right]^n\left[\frac{\eta-\sqrt{\eta^2-4m}}{\sqrt{\eta^2-4m}}\right]^{1/2}$$
$$\left.\times e^{-i\Theta}\exp\left(-\frac{1}{4\varepsilon}(2m-\eta\sqrt{\eta^2-4m})\right)\right\}$$
$$\times\frac{\alpha_0}{\sqrt{2}}\left(\frac{\partial\eta}{\partial X}\right)^{-1/2}\exp\left(\frac{i}{\varepsilon}\int_{X_0}^{X}k_0(s)\,ds\right). \qquad (B\,12)$$

We note that equation (B 12) can be written as the superposition $\psi^+ + \psi^-$ of two distinct contributions ψ^+ and ψ^-, which can be constructed from (5.1) by substituting $I_\varepsilon^{(n)+}(\eta)$ and $I_\varepsilon^{(n)-}(\eta)$ defined in (B 5) into the expressions (B 2 *a*,b) for V and V'. The resulting functions $\psi^+(X;\omega_{g_n},\varepsilon)$ and $\psi^-(X;\omega_{g_n},\varepsilon)$ take the form of local WKBJ approximations pertaining to spatial branches $k^+(X;\omega_{g_n})$ and $k^-(X;\omega_{g_n})$, respectively. When the condition $I_\varepsilon^{(n)+}(\eta)/I_\varepsilon^{(n)-}(\eta)=O(1)$, equivalently

$$\mathrm{Re}\{f(r^+(\eta);\eta)-f(r^-(\eta);\eta)\}=\mathrm{Im}\left[\int_{2\sqrt{m}}^{\eta}\sqrt{4m-s^2}\,ds\right]=0,$$

is fulfilled, both approximations ψ^+ and ψ^- become of the same order of magnitude, as one would expect on a Stokes line. Furthermore, one can easily show that $\mathrm{Re}[f(r^+(\eta);\eta)]-\mathrm{Re}[f(r^-(\eta);\eta)]>0$ in regions $\eta(+;\omega_{g_n})$ and $\eta(-;\omega_{g_n})$, provided that the square root is defined according to (B 6). Approximation (B 10) for $\psi(X;\omega_{g_n},\varepsilon)$ then coincides with $\psi^+(X;\omega_{g_n},\varepsilon)$ in regions $\eta(+;\omega_{g_n})$ and $\eta(-;\omega_{g_n})$ and it is therefore subdominant. Following classical properties of the Stokes phenomenon, this subdominant WKBJ approximation remains valid in neighbouring sectors of the complex η plane where it now becomes dominant.

Appendix C. Type-2 global eigenfunctions

This appendix is concerned with the reduction of uniform approximation (5.38) obtained for type-2 global modes.

Note first that when $\eta(X;\omega_{g_n})=O(\sqrt{\varepsilon})$, i.e. when X is close to the double-turning point X_s and satisfies $|X-X_s|=O(\sqrt{\varepsilon})$, two simplifications immediately occur: the second term in (5.38) becomes negligible with respect to the first and expression (A 3 *a*, *b*) for $B_0(X;\omega_{g_n})$ reduces to

$$B_0(X,\omega_{g_n})\sim\alpha_0\left(\frac{\partial\eta}{\partial X}(X;\omega_{g_n})\right)^{-1/2},$$

Θ being $O(\sqrt{\varepsilon})$ when $|X-X_s|=O(\sqrt{\varepsilon})$. If, in addition, (5.29) is used to replace $\eta(X;\omega_{g_n})$ by its leading-order approximation $\eta(X;\omega_s)$, expression (5.38) may be

written as

$$\psi(X;\omega_{g_n},\varepsilon)\sim\alpha_0\left(\frac{\partial\eta}{\partial X}(X;\omega_s)\right)^{-1/2}\mathrm{He}_n\left[\frac{\eta(X;\omega_s)}{\sqrt{\varepsilon}}\right]\times\exp\left(-\frac{\eta^2(X;\omega_{g_n})}{4\varepsilon}\right)\exp\left(\frac{\mathrm{i}}{\varepsilon}\int_{X_s}^{X}k_0(s)\,\mathrm{d}s\right).\quad(\mathrm{C}\,1)$$

Note that $\eta(X;\omega_{g_n})$ has not been replaced by $\eta(X;\omega_s)$ in the exponent of (C 1) because the $O(\varepsilon)$ correction induces an $O(1)$ amplitude correction as shown below.

When $\eta(X;\omega_{g_n})\gg\sqrt{\varepsilon}$, i.e. when X is at a distance larger than $O(\sqrt{\varepsilon})$ from the double-turning point X_s, the second term in (5.38) is no longer negligible but nevertheless the expression of $V_n'(\eta/\sqrt{\varepsilon})$ can be simplified. When $\eta(X;\omega_{g_n})\gg\sqrt{\varepsilon}$, using again (5.29), one can immediately show that

$$V_n'\left[\frac{\eta(X;\omega_{g_n})}{\sqrt{\varepsilon}}\right]\sim-\frac{\eta(X;\omega_s)}{2\sqrt{\varepsilon}}\mathrm{He}_n\left[\frac{\eta(X;\omega_s)}{\sqrt{\varepsilon}}\right]\exp\left(-\frac{\eta^2(X;\omega_{g_n})}{4\varepsilon}\right).$$

Expression (5.38) is then written as

$$\psi(X;\omega_{g_n},\varepsilon)\sim\mathrm{He}_n\left[\frac{\eta(X;\omega_s)}{\sqrt{\varepsilon}}\right]\{B_0(X;\omega_s)-\tfrac{1}{2}\eta(X;\omega_s)C_0(X;\omega_s)\}\times\exp\left(-\frac{\eta^2(X;\omega_{g_n})}{4\varepsilon}\right)\exp\left(\frac{\mathrm{i}}{\varepsilon}\int_{X_0}^{X}k_0(s)\,\mathrm{d}s\right).\quad(\mathrm{C}\,2)$$

The expression within braces takes a simpler form if one appeals to the relation

$$\mathrm{i}\eta(X;\omega_s)\frac{\partial\eta}{\partial X}(X;\omega_s)=2\sqrt{R_0(X;\omega_s)},$$

obtained by differentiating (5.30) with respect to X, and if expressions (A 3 a,b) for $B_0(X;\omega)$ and $C_0(X;\omega)$ are invoked. The intermediate result then reads

$$\{B_0(X;\omega_s)-\tfrac{1}{2}\eta(X;\omega_s)C_0(X;\omega_s)\}=\alpha_0\left(\frac{\partial\eta}{\partial X}(X;\omega_s)\right)^{-1/2}\exp(\mathrm{i}\Theta(X;\omega_s)).$$

It therefore follows that

$$\psi(X;\omega_{g_n},\varepsilon)\sim\alpha_0\left(\frac{\partial\eta}{\partial X}(X;\omega_s)\right)^{-1/2}\mathrm{He}_n\left[\frac{\eta(X;\omega_s)}{\sqrt{\varepsilon}}\right]\exp(\mathrm{i}\Theta(X;\omega_s))\times\exp\left(-\frac{\eta^2(X;\omega_{g_n})}{4\varepsilon}\right)\exp\left(\frac{\mathrm{i}}{\varepsilon}\int_{X_0}^{X}k_0(s)\,\mathrm{d}s\right).\quad(\mathrm{C}\,3)$$

Recall that $\Theta(X;\omega_s)$ is given by (A 4) in Appendix A and satisfies $\Theta(X_s;\omega_s)=0$. Approximation (C 3) expanded near X_s then gives exactly the same result as (C 1) for the global mode in the region $|X-X_s|=O(\sqrt{\varepsilon})$. Thus, (C 3) remains valid for all X and can be considered as a uniform leading-order approximation.

It remains to evaluate the exponential factor of $\exp(-\eta^2(X;\omega_{g_n})/4\varepsilon)$ when $\varepsilon\to0$. Using expansion (5.17) for ω_{g_n}, $\eta^2(X;\omega_{g_n})$ can be approximated by its Taylor expansion around ω_s to give

$$\exp\left(-\frac{\eta^2(X;\omega_{g_n})}{4\varepsilon}\right)\sim\exp\left(-\frac{\eta^2(X;\omega_s)}{4\varepsilon}\right)\exp\left(-\frac{\omega_{g_n}^{(1)}}{4}\frac{\partial(\eta^2)}{\partial\omega}(X;\omega_s)\right).\quad(\mathrm{C}\,4)$$

Both $\eta(X;\omega_s)$ and $\omega_{g_n}^{(1)}$ have already been calculated as (5.30) and (5.35), respectively. An expression for $(\partial(\eta^2)/\partial\omega)(X;\omega_s)$ has not yet been obtained and its computation requires a little algebra, as outlined in the rest of this appendix.

An expression involving $(\partial\eta/\partial\omega)(X;\omega)$ is generated by differentiating (5.5) with respect to ω:

$$\frac{\partial\eta}{\partial\omega}(X;\omega)\sqrt{\eta^2(X;\omega)-\eta_1^2(\omega)}+\frac{\partial(\eta_1^2)}{\partial\omega}(\omega)\int_{\eta_0}^{\eta(X;\omega)}\frac{\mathrm{d}s}{2\sqrt{s^2-\eta_1^2(\omega)}}$$
$$=2\int_{X_0}^{X}\frac{1}{\omega_{kk}(r)}\sqrt{\frac{\omega_{kk}(r)}{2(\omega_0(r)-\omega)}}\,\mathrm{d}r. \qquad (C\,5)$$

This functional equation is independent of the definitions chosen for the various square roots, provided that the branches of the square roots appearing on the left-hand side of (C 5) are the images of those on the right-hand side through the mapping $X\mapsto\eta(X;\omega)$. However, the contour of integration should not cross any branch cut. A convenient selection of X_0 and of the integration path may have to be made in order to have that property satisfied. At the value $\omega=\omega_s$, the first term of (C 5) reduces to $\frac{1}{2}(\partial(\eta^2)/\partial\omega)(X;\omega_s)$. In addition, $\eta_1(\omega_s)$ is zero and, according to relations (5.4) and (5.34) with $\varsigma=1$, $(\partial(\eta_1^2)/\partial\omega)(\omega_s)$ is equal to

$$\frac{4}{\omega_{kk}^s}\sqrt{\frac{\omega_{kk}^s}{\omega_{0XX}^s}}.$$

One may then obtain from (C 5) the following expression:

$$\frac{\partial(\eta^2)}{\partial\omega}(X;\omega_s)=4\int_{X_0}^{X}\frac{1}{\omega_{kk}(r)}\sqrt{\frac{\omega_{kk}(r)}{2(\omega_0(r)-\omega_s)}}\,\mathrm{d}r-\frac{4}{\omega_{kk}^s}\sqrt{\frac{\omega_{kk}^s}{\omega_{0XX}^s}}\int_{\eta_0}^{\eta(X;\omega_s)}\frac{\mathrm{d}s}{s}. \qquad (C\,6)$$

The second integral has voluntarily not been replaced by a logarithmic function because its value varies according to the number of complete 2π rotations made by the contour of integration around the origin. To get a single-valued expression for that integral, a branch cut issuing from the origin should be selected in the η plane, the contour of integration in the η plane being required not to cross it. The contour of integration in the X plane for the first integral in (C 6) is the preimage of the previous contour through the mapping $X\mapsto\eta(X;\omega_s)$ and it suffers from similar restrictions. The first integral taken separately, is also multivalued and depends on the number of rotations completed around X_s. Since the integration path from η_0 to η in the second integral is the image by $X\mapsto\eta(X;\omega_s)$ of the integration path from X_0 to X in the first integral, the sum of both integrals is, therefore, single-valued. Finally, in view of the relation

$$\frac{\partial(\eta_1^2)}{\partial\omega}(\omega)\int_{\eta_0}^{\eta_1(\omega)}\frac{1}{2\sqrt{s^2-\eta_1^2(\omega)}}\,\mathrm{d}s=2\int_{X_0}^{X_1(\omega)}\frac{1}{\omega_{kk}(r)}\sqrt{\frac{\omega_{kk}(r)}{2(\omega_0(r)-\omega)}}\,\mathrm{d}r,$$

valid for any ω including ω_s, the function $(\partial(\eta^2)/\omega)(X;\omega_s)$ defined by (C 6) can be continuously extended to X_s as

$$\frac{\partial(\eta^2)}{\partial\omega}(X_s;\omega_s)=0.$$

References

Anyanwu, D. U. & Keller, J. B. 1975 Asymptotic solutions of eigenvalue problems for second-order ordinary differential equations. *Communs Pure Appl. Math.* **28**, 753–763.

Bender, C. M. & Orszag, S. A. 1978 *Advanced mathematical methods for scientists and engineers.* New York: McGraw-Hill.

Bers, A. 1983 Space-time evolution of plasma instabilities −absolute and convective. In *Handbook in plasma physics* (ed. M. N. Rosenbluth & R. Z. Sagdeev), vol. 1, pp. 451–517. Amsterdam: North-Holland.

Bar-Sever, Y. & Merkine, L. O. 1988 Local instabilities of weakly non-parallel large scale flows: WKB analysis. *Geophys. Astrophys. Fluid Dyn.* **41**, 233–286.

Chomaz, J. M., Huerre, P. & Redekopp, L. G. 1988 Bifurcations to local and global modes in spatially developing flows. *Phys. Rev. Lett.* **60**, 25–28.

Chomaz, J. M., Huerre, P. & Redekopp, L. G. 1990 Effect of nonlinearity and forcing on global modes. In *Proc. Conf. on New Trends in Nonlinear Dynamical Systems and Pattern-forming Phenomena: The Geometry of Nonequilibrium. NATO ASI Series B: Physics* (ed. P. Coullet & P. Huerre), vol. 37, pp. 259–274. New York: Plenum.

Chomaz, J. M., Huerre, P. & Redekopp, L. G. 1991 A frequency selection criterion in spatially-developing flows. *Stud. Appl. Math.* **84**, 119–144.

DiPrima, R. C. & Stuart, J. T. 1972 Non-local effects in the stability of flow between eccentric rotating cylinders. *J. Fluid Mech.* **54**, 393–415.

Drazin, P. G. 1974*a* On a model of instability of a slowly-varying flow. *Q. Jl Mech. Appl. Math.* **27**, 69–86.

Drazin, P. G. 1974*b* Kelvin–Helmholtz instability of a slowly varying flow. *J. Fluid Mech.* **65**, 781–797.

Eckelmann, H., Graham, J. M. R., Huerre, P. & Monkewitz, P. A. 1993 *Bluff-body wakes, dynamics and instabilities, IUTAM Symp.* Berlin: Springer.

Gent, P. R. 1976 Baroclinic instability of a slowly varying zonal flow. *J. Atmos. Sci.* **31**, 1983–1994.

Gent, P. R. & Leach, H. 1976 Baroclinic instability in an eccentric annulus. *J. Fluid Mech.* **77**, 769–788.

Hannemann, K. & Oertel Jr, H. 1989 Numerical simulation of the absolutely and convectively unstable wake. *J. Fluid Mech.* **199**, 55–88.

Huerre, P. & Monkewitz, P. A. 1990 Local and global instabilities in spatially developing flows. *A. Rev. Fluid Mech.* **22**, 473–537.

Hunt, R. E. 1995 Spatially varying flows with localized forcing. Ph.D. thesis, Trinity College, Cambridge.

Hunt, R. E. & Crighton, D. G. 1991 Instability of flows in spatially developing media. *Proc. R. Soc. Lond.* A **435**, 109–128.

Karniadakis, G. E. & Triantafyllou, G. S. 1989 Frequency selection and asymptotic states in laminar wakes. *J. Fluid Mech.* **199**, 441–469.

Koch, W. 1985 Local instability characteristics and frequency determination of self-excited wake flows. *J. Sound Vib.* **99**, 53–83.

Langer, R. E. 1949 The asymptotic solutions of ordinary linear differential equations of the second-order, with special reference to a turning point. *Trans. Am. Math. Soc.* **67**, 461–490.

Le Dizès, S., Monkewitz, P. A. & Huerre, P. 1991 Weakly nonlinear analysis of spatially-developing shear flows. *Bull. Am. Phys. Soc.* **36**, 2675.

Le Dizès, S., Huerre, P., Chomaz, J. M. & Monkewitz, P. A. 1993 Nonlinear stability analysis of slowly-diverging flows: Limitations of the weakly nonlinear approach. In *Proc. IUTAM Symp. on Bluff-Body Wakes, Dynamics and Instabilities* (ed. H. Eckelmann, J. M. R. Graham, P. Huerre & P. A. Monkewitz), pp. 147–152. Berlin: Springer.

Lynn, R. Y. S. & Keller, J. B. 1970 Uniform asymptotic solutions of second-order linear ordinary differential equations with turning points. *Communs Pure Appl. Math.* **23**, 379–408.

McKelvey, R. N. 1955 The solutions of second-order linear ordinary differential equations about turning points of order two. *Trans. Am. Math. Soc.* **79**, 103–123.

PHILOSOPHICAL TRANSACTIONS OF THE ROYAL SOCIETY A MATHEMATICAL, PHYSICAL & ENGINEERING SCIENCES

Mathis, C., Provansal, M. & Boyer, L. 1984 The Bénard-von Kármán instability: an experimental study near the threshold. *J. Phys., Paris Lett.* **45**, 483–491.

Monkewitz, P. A. 1988 The absolute and convective nature of instability in two-dimensional wakes at low Reynolds numbers. *Physics Fluids* **31**, 999–1006.

Monkewitz, P. A. 1990 The role of absolute and convective instability in predicting the behaviour of fluid systems. *Eur. J. Mech. B: Fluids* **9**, 395–413.

Monkewitz, P. A., Bechert, D. W., Lehmann, B. & Barsikow, B. 1990 Self-excited oscillations and mixing in heated round jets. *J. Fluid Mech.* **213**, 611–639.

Monkewitz, P. A., Huerre, P. & Chomaz, J. M. 1993 Global linear stability analysis of weakly non parallel shear flows. *J. Fluid Mech.* **251**, 1–20.

Monkewitz, P. A. & Sohn, K. D. 1988 Absolute instability in hot jets. *AIAA Jl* **26**, 911–916.

Newell, A. C., Passot, T. & Lega, J. 1993 Order parameter equations for patterns. *A. Rev. Fluid Mech.* **25**, 399–453.

Papageorgiou, O. 1987 Stability of the unsteady viscous flow in a curved pipe. *J. Fluid Mech.* **182**, 209–233.

Pierrehumbert, R. T. 1984 Local and global baroclinic instability of zonally varying flow. *J. Atmos. Sci.* **41**, 2141–2162.

Pesenson, M. Z. & Monkewitz, P. A. 1993 Frequency selection and global instabilities in three-dimensional weakly nonparallel flows. *Phys. Rev. Lett.* **70**, 2722–2725.

Pokrovskii, V. L. & Khalatnikov, I. M. 1961 On the problem of above-barrier reflection of high-energy particles. *Soviet Phys. JETP* **13**, 1207–1210.

Schär, C. & Smith, R. B. 1993 Shallow-water flow past isolated topography. Part II. Transition to vortex shedding. *J. Atmos. Sci.* **50**, 1401–1428.

Sibuya, Y. 1975 Global theory of a second order linear ordinary differential equation with a polynomial coefficient. *Mathematics studies*, vol. 18. Amsterdam: North-Holland.

Soward, A. M. & Jones, C. A. 1983 The linear stability of the flow within narrow gap between two concentric rotating spheres. *Q. Jl Mech. Appl. Math.* **36**, 19–42.

Soward, A. M. 1992 Thin disc kinematic $\alpha\omega$-dynamo models. II. Short length scale modes. *Geophys. Astrophys. Fluid Dyn.* **64**, 201–225.

Sreenivasan, K. R., Raghu, S. & Kyle, D. 1989 Absolute instability in variable density round jets. *Exp. Fluids* **7**, 309–317.

Strykowski, P. J. & Sreenivasan, K. R. 1990 On the formation and suppression of vortex 'shedding' at low Reynolds numbers. *J. Fluid Mech.* **218**, 71–107.

Strykowski, P. J. & Niccum, D. L. 1991 The stability of countercurrent mixing layers in circular jets. *J. Fluid Mech.* **227**, 309–343.

Wasow, W. 1985 *Linear turning point theory.* New York: Springer.

Received 8 November 1993; revised 28 July 1994; accepted 28 February 1995

PHILOSOPHICAL TRANSACTIONS OF THE ROYAL SOCIETY A MATHEMATICAL, PHYSICAL & ENGINEERING SCIENCES